Journal of Asthma and Allergy

Dovepress
Taylor & Francis Group

Open Access Full Text Article

ORIGINAL RESEARCH

Glucagon-Like Peptide 1 Receptor (*Glp1r*) Deficiency Does Not Appreciably Alter Airway Inflammation or Gut-Lung Microbiome Axis in a Mouse Model of Obese Allergic Airways Disease and Bariatric Surgery

Yeon Ji Kim[1,*], Victoria M Ihrie[2,*], Pixu Shi[3], Mark D Ihrie[2], Jack T Womble[2], Anna Hill Meares[1], Joshua A Granek[3], Claudia K Gunsch[1], Jennifer L Ingram[2]

[1]Department of Civil and Environmental Engineering, Pratt School of Engineering, DukeUniversity, Durham, NC, USA; [2]Division of Pulmonary, Allergy and Critical Care Medicine, Department of Medicine, Duke University Medical Center, Durham, NC, USA; [3]Biostatistics and Bioinformatics, Division of Integrative Genomics, Department of Medicine, Duke University Medical Center, Durham, NC, USA

*These authors contributed equally to this work

Correspondence: Jennifer L Ingram, Department of Medicine, Duke University Medical Center, Box 2641 DUMC, 203 Research Drive, Durham, NC, 27710, USA, Tel +1 919-668-1439, Email jennifer.ingram@duke.edu

Purpose: High body mass index (≥30 kg/m^2) is associated with asthma severity, and nearly 40% of asthma patients exhibit obesity. Furthermore, over 40% of patients with obesity and asthma that receive bariatric surgery no longer require asthma medication. Increased levels of glucagon-like peptide 1 (GLP-1) occur after bariatric surgery, and recent studies suggest that GLP-1 receptor (GLP-1R) signaling may regulate the gut microbiome and have anti-inflammatory properties in the lung. Thus, we hypothesized that increased GLP-1R signaling following metabolic surgery in obese and allergen-challenged mice leads to gut/lung microbiome alterations, which together contribute to improved features of allergic airways disease.

Methods: Male and female *Glp1r*-deficient (*Glp1r*$^{-/-}$) and replete (*Glp1r*$^{+/+}$) mice were administered high fat diet (HFD) to induce obesity with simultaneous intranasal challenge with house dust mite (HDM) allergen to model allergic airway disease with appropriate controls. Mice on HFD received either no surgery, sham surgery, or vertical sleeve gastrectomy (VSG) on week 10 and were sacrificed on week 13. Data were collected with regard to fecal and lung tissue microbiome, lung histology, metabolic markers, and respiratory inflammation.

Results: HFD led to metabolic imbalance characterized by lower GLP-1 and higher leptin levels, increased glucose intolerance, and alterations in gut microbiome composition. Prevalence of bacteria associated with short chain fatty acid (SCFA) production, namely *Bifidobacterium, Lachnospiraceae UCG-001*, and *Parasutterella*, was reduced in mice fed HFD and positively associated with serum GLP-1 levels. Intranasal HDM exposure induced airway inflammation. While *Glp1r*$^{-/-}$ genotype affected fecal microbiome beta diversity metrics, its effect was limited.

Conclusion: Herein, GLP-1R deficiency had surprisingly little effect on host gut and lung microbiomes and health, despite recent studies suggesting that GLP-1 receptor agonists are protective against lung inflammation.

Plain Language Summary: Asthma is a chronic lung disease that affects over 20 million Americans. In addition, obesity is a major worldwide healthcare problem whose impact is increasing each year. Asthma patients with obesity have worse symptoms, use more medications and have reduced asthma control than lean patients. Also, both asthma and obesity are linked to changes in the normal bacteria that live in the gut and the airways. Weight loss, either through bariatric surgery or through diet and exercise, improves asthma symptoms, through unknown mechanisms. One way that bariatric surgery may impact asthma is through the increase in beneficial gut hormones (GLP-1) and restoration of altered bacteria in the gut and airways. Our study shows that overall, obese mice experience changes in hormones involved in weight gain and glucose metabolism as well as gut bacteria, particularly those that may produce

Received: 28 May 2024
Accepted: 22 January 2025
Published: 27 February 2025

important factors that could improve health. We did not find any links between changes in the bacteria in the gut or lung and features of airway disease or effects from bariatric surgery in the mice. Mice that lacked GLP-1 activity did not differ from normal mice for weight, glucose tolerance, or prevalence of bacteria in the lung. Future studies will explore the timeline of these bacterial changes and the role of the gut and lung microbiomes in human obesity-associated asthma.

Keywords: vertical sleeve gastrectomy, allergic airways disease, short-chain fatty acids, gut-lung microbiome axis

Introduction

Asthma is a heterogenous chronic disease characterized by airway hyperresponsiveness (AHR), inflammation, and remodeling.[1] Nearly 40% of asthma patients in the US are diagnosed with comorbid obesity.[2] Patients who exhibit asthma with comorbid obesity are at a higher risk for severe disease, and increasing body mass index (BMI) is associated with severe asthma.[3–5] Asthma phenotypes associated with obesity include: early-onset asthma (<12 years of age) with adult-onset obesity, versus late-onset asthma (≥12 years of age) in people with existing obesity.[1,6] Herein, we focus on the early-onset asthma phenotype, which is characterized by Type 2 (T2) cytokine-mediated airway inflammation[7] and is related to immunological sensitization of environmental allergens such as pollen, molds, pet dander or house dust mite (HDM) allergen.[8]

Interestingly, patients with obesity and asthma that undergo bariatric surgery present improved asthma outcomes for up to three years post-operation, leading to reduced asthma medication use.[9–12] Furthermore, over 40% of these patients no longer require medication to manage asthma symptoms after bariatric surgery.[13,14] While weight loss is associated with reduced asthma symptoms, this phenomenon is not captured by weight loss alone, as asthma medication use is reduced as soon as one month post-operation, before significant weight loss occurs.[9,12] Instead, obesity likely contributes to worsened asthma symptoms via a multitude of mechanisms. Physical mechanisms include restriction of the thoracic cavity by adipose tissue, contributing to changes in chest wall and lung mechanics.[15] Obesity is also associated with prevalence of metabolic syndrome, and each of its criteria (abdominal adiposity, dyslipidemia, hyperglycemia, hypertension, and low blood high-density lipoprotein) has been associated with asthma.[16]

The gut microbiome, an important health regulator, is also perturbed in obesity, which could have systematic effects on the immune system as gut microbiota can produce immunomodulatory metabolites such as short chain fatty acids (SCFAs).[17–20] In addition to the gut, the human lung also harbors a dynamic microbiome that is characterized by constant influx and efflux of microbiota in health.[21] Increasing evidence supports that the gut and lung microbiomes can communicate and affect each other, potentially through circulating metabolites such as SCFAs, and this cross-talk is termed the gut-lung microbiome axis.[16] However, few studies have characterized the gut and lung microbiome axis in obesity and/or asthma,[22,23] even after Michalovich et al[22] reported that obesity and asthma have additive effects on microbiome dysbiosis in the gut and the lung. This knowledge gap is important, especially in the context of asthma with comorbid obesity, as studies report persistent changes in gut microbiome following bariatric surgery, but their impact on asthma symptoms remain largely unknown.[24–30]

A hormone that potentially connects obesity, asthma, and bariatric surgery is glucagon-like peptide-1 (GLP-1). This pleiotropic hormone stimulates insulin secretion, satiety, and lipolysis, and has been suggested as a regulator of the gut microbiome. Furthermore, GLP-1 receptor agonists (GLP1-RA) have gained popularity in recent years as part of a weight loss regimen.[31] Recent research using GLP-1RA suggests that GLP-1 confers protection against lung inflammation.[32–35] Importantly, decreased circulating GLP-1 levels are reported in obesity, and this imbalance is remediated following bariatric surgery.[36–38] However, if and how these restored circulating GLP-1 levels contribute to the microbiome changes or asthma symptoms after bariatric surgery remains a knowledge gap.

Bariatric surgery can be modeled in rodents using a modified vertical sleeve gastrectomy (VSG).[39,40] Obesity in rodents is generally diet-induced,[41] and can have significant effects on immune responses, airway hyperresponsiveness, and the gut microbiome.[42–44] Furthermore, gut microbiome changes occur in rodents after bariatric surgery.[45,46] Therefore, we tested the hypothesis that increased GLP-1R signaling after bariatric surgery leads to improved allergen-induced airway inflammation by modulating the gut-lung microbiome axis in a murine loss-of-function and intervention model.

Materials and Methods

Animals

For this study, *Glp1r*-deficient (*Glp1r*$^{-/-}$) and -replete (*Glp1r*$^{+/+}$) littermates on the C57BL/6J background were bred in collaboration with the Duke University Research Animal Breeding Core, and cohorts of mice of mixed genotype, mixed sex, and aged 6–8 weeks were selected (total n = 91 mice). All mice were housed 5 mice/cage in micro-isolator cages on corn cob bedding in pathogen-free facilities at Duke University. Mice were fed either high fat diet (HFD; 60% kcal by fat, Research Diets, #D12492i, Lot #22051604i) for 10 weeks to induce obesity and glucose intolerance or normal chow (15% kcal by fat, LabDiet, #5053) for the control group. Both diets were administered to mice ad libitum. Concurrently, mice were sensitized with 50 µg of house dust mite allergen (HDM, Greer Laboratories, #XPB91D3A2.5, Lot 381018) or saline (control, Gibco, #10010-023) three times per week for the first two weeks. They then had 4 weeks of break followed by 4 weeks of inducing allergic airway disease via intranasal instillation of HDM or saline (control) three times per week.

At week 10, a cohort of mice fed HFD underwent vertical sleeve gastrectomy or sham surgery as previously reported.[3] A different cohort from both diets was sacrificed for pre-surgery lung tissue microbiome samples (n = 15). Regardless of surgery status, all mice were fed powdered normal chow mixed with water for 1 week after surgery. On week 12, mice again underwent intranasal challenge with HDM or saline and were given their original diets. Mice were sacrificed in week 13 for collection of lung tissue and bronchoalveolar lavage fluid (BALF). Body weight was recorded at weeks 0, 10, and 13. Each subgroup based on diet, intranasal challenge, and surgery status had at least 5 mice surviving at sacrifice. The study was approved by Duke Institutional Animal Care and Use Committee (IACUC) (A041-20-02) and conducted in accordance with the American Association for the Accreditation of Laboratory Animal Care guidelines. The study design is summarized in Figure 1.

Glucose Tolerance Test

Glucose tolerance was measured at week 0 (pre-treatment), week 10 (pre-surgery), and week 12 (post-surgery). Mice were fasted for 5 hours, and then a 200 µL bolus of 10% glucose (Sigma, #G8644) was delivered via oral gavage using a curved feeding needle (Kent Scientific, #FNC-20-1.5). Mice were placed in a restraint (Braintree Scientific, #TV-150) and blood was collected from the tail vein. Blood glucose was measured pre-gavage, and at 10-, 30-, and 90-minutes post-gavage using an Accu-chek Performa glucose meter (Roche).

Lung and Gut Microbiome Sample Collection

When possible, at least one fecal pellet was collected from each mouse during glucose testing at weeks 0 and 10 through voluntary defecation. At sacrifice, fecal pellets were collected by gentle massaging of the intestine to remove feces. All fecal samples were stored at −80°C until DNA extraction. At the end of the experiment (Week 13), a subset of mice (n = 48) was sacrificed via lethal injection and the entirety of the left and right lung were excised for microbiome analysis. Tissue was placed on ice in 1 mL sterile water in a round-bottomed test tube and mechanically homogenized using a Tissue Tearor immersion blender (Biospec Products, Inc., model 985370–395) for 3 seconds at 20,000 revolutions per minute (rpm) repeated 3 times. The blender probe was washed between each sample by submerging in 70% ethanol and running at 25,000 rpm for 10 seconds, and then again in deionized water before blotting with a paper towel. Sample collection controls of sterile water were also subjected to the blending protocol. After homogenization, samples were transferred to a 2 mL Dolphin tube (VWR, #490010-618) and centrifuged at 13,000 rpm for 30 min at 4°C. Supernatants were removed and pellets were snap-frozen in liquid nitrogen before storage at −80°C.

Bronchoalveolar Lavage Fluid Collection

Twenty-four hours after the last intranasal treatment, mice that were not sacrificed for microbiome analysis lung tissue collection were used for collecting BALF and lung tissue for histopathology (n = 43). A blood-draw from the inferior vena cava served as confirmation of sacrifice, and BALF was collected via gentle instillation and withdrawal of 1 mL phosphate buffered saline (PBS) 3 times. Once the BALF was collected, the right lung was tied at the bronchus and the medial, and the lower and accessory lobes were excised and snap-frozen in liquid nitrogen. The remaining left lung was gently inflated with

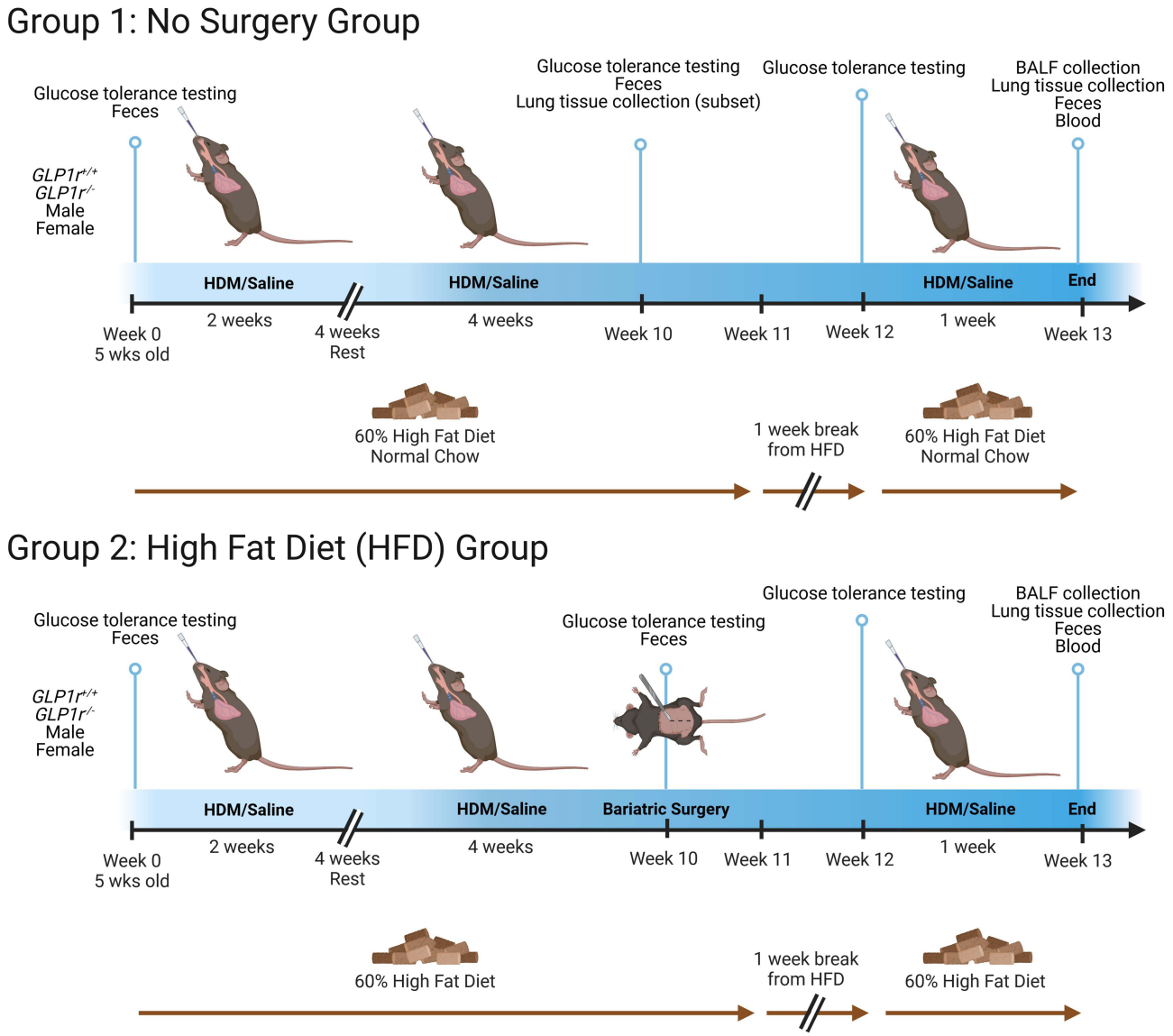

Figure 1 Mouse study design with glucagon-like peptide-1 receptor deficient ($Glp1r^{-/-}$) and replete ($Glp1r^{+/+}$) littermates. High fat diet (HFD) induces obesity and glucose intolerance, and house dust mite (HDM) induces allergic airway inflammation (n = 91). At sacrifice, either lung tissue (n = 48) or bronchoalveolar lavage fluid (BALF) collection was performed (n = 43).

10% formalin and tied off at the bronchus, and the bronchial tree, heart, and left lung were excised in one piece and placed into a round-bottom tube filled with 5 mL 10% formalin. Left lungs were excised from the bronchus after 24 hours and placed bronchus-down into plastic cassettes and stored in 70% ethanol in preparation for paraffin embedding.

Lung Histopathology

Lungs were paraffin-embedded, and 5 µm sections were mounted on slides. Slides were stained with either hematoxylin and eosin (H&E), Periodic Acid-Schiff (PAS) or Masson's Trichrome stains. Histological scoring was performed as described in Ihrie et al.[47]

BALF Differential Immune Cell Counting

BALF was centrifuged at 1200 rpm for 10 min at 4°C and supernatant was removed. Cell pellets were resuspended in 500 µL red blood cell lysis buffer (Invitrogen, #00430054) for 5 min on ice before centrifuging again. Pellet was resuspended in 500 µL PBS and cells were counted using a Cellometer K2 (Nexcelom Bioscience). A total of 25,000

cells per sample were mounted on slides via a Cytospin 4 (Thermo Fisher Scientific) at 800 rpm for 3 minutes. Slides were allowed to air dry overnight before staining with EasyIII stain (Azer Scientific, #ES904, ES905, ES906). Differential counts were determined by imaging slides at 10x magnification and counting the number of macrophages, neutrophils, eosinophils, lymphocytes, and epithelial cells. 200–250 cells were scored per slide.

Serum Protein Measurements

Proteins of interest were measured in the serum using the U-PLEX Obesity Combo 2 (mouse) kit (MesoScale Discovery, #K15301K-1) according to manufacturer's protocol. All samples were diluted 1:4.

Microbiome Sample DNA Extraction and Sequencing Data Generation

DNA from fecal samples were extracted with DNeasy PowerSoil Pro kit (QIAGEN, #47014) according to the manufacturer's instructions. DNA extraction blanks and elution buffer blanks were included (n = 12 and 8, respectively). Lung tissue samples were processed using DNeasy Blood & Tissue kit (QIAGEN, #69504) with a modified protocol as previously described.[48,49] Briefly, deviations from the manufacturer's instructions were: doubling the amount of proteinase K (QIAGEN, #19131) to 40 µL in the lysis step, bead-beating samples with a PowerLyzer 24 homogenizer (QIAGEN) using PowerBead Pro tubes (QIAGEN, #19301) for 1 minute at 2800 rpm, and eluting DNA twice with 100 µL of elution buffer each time. DNA extraction and elution buffer blanks were included (n = 4 each).

Extracted DNA was quantified with Qubit 2.0 fluorometer and stored at −20°C until use. Lung tissue DNA samples were submitted to Duke Microbiome Center to prepare libraries for sequencing. 16S rRNA gene hypervariable region 4 (v4) was amplified in triplicates following Earth Microbiome Project (EMP) protocol with standard EMP v4 primers 515F (5'- GTGYCAGCMGCCGCGGTAA-3') and 806Rb (5'- GGACTACNVGGGTWTCTAAT-3') for a total of 35 polymerase chain reaction (PCR) cycles.[50] Two no-template controls for PCR and a positive control (ZymoBIOMICS gut microbiome standard, Zymo Research, #D6331-A) were included. Triplicate samples were merged at magnetic bead clean-up step, quantified on a GloMax microplate reader (Promega), and equimolar PCR products were pooled for sequencing.

Fecal DNA was diluted to either 3 or 15 ng/µL to normalize input DNA amount to 15 ng for PCR. Sterile molecular biology grade water used in dilutions was included as blanks in triplicates. Libraries were prepared following standard Illumina 16S amplicon guidelines using 515F and 806Rb primers with dual-indexed barcoding.[51] A total of 33 cycles of PCR was performed with Platinum *Taq* polymerase (Invitrogen, #15966005) with the annealing temperature modified to 60°C. PCR products were quantified on Qubit 2.0 fluorometer (Thermo Fisher), and equimolar PCR products were pooled for sequencing. The final fecal pool and lung tissue pool were submitted to Duke Sequencing and Genomic Technologies (SGT) shared resource, and quantitative PCR was performed to determine the input amount for each pool. The combined pool was sequenced on an Illumina MiSeq instrument with v2 chemistry (250 base pairs, paired-end).

Sequencing Data Analysis

Sequencing data was analyzed in R programming suite (v4.3.0). Raw reads were processed through DADA2 pipeline (v1.28.0)[52] with SILVA v138 database.[53,54] Potential reads from contamination were identified and removed using procedural blanks with *decontam* package (v1.14.0)[55] using method = "either" with thresholds 0.1 and 0.5 for frequency test and prevalence test, respectively. Samples that had less than 1000 reads after *decontam* were excluded from further analysis and a phylogenetic tree was constructed with Randomized Axelerated Maximum Likelihood (RAxML) v8.2.12.[56] Alpha diversity metrics (Shannon diversity,[57] observed richness, and Faith's phylogenetic distance [PD])[58] were calculated with packages *phyloseq* (v1.44.0)[59] and *picante* (v1.8.2).[60] Weighted and unweighted unique fraction metric (UniFrac) distances[61] were calculated with package *vegan* (v2.6.4)[62] and visualized as principal coordinate analysis (PCoA) plots using the top two principal coordinates. Code used in analysis is publicly available on GitHub as listed below.

Statistical Analysis

All statistical analyses were performed in R (v4.3.0) using package *Rstatix* (v0.7.2) unless otherwise stated. Mice were divided into two groups for data analyses: 1) mice that did not undergo any surgery (no surgery group) to test for the

effect of diet and 2) mice that were fed HFD (HFD group) to test for the effect of surgery. As such, mice that were fed HFD and did not receive surgery were included in both analyses. Since these mice were compared to different groups for different research questions, multiple-testing correction was not applied for including this group twice. Confounding variables considered in both analyses included intranasal treatment, sex, and genotype. More details on each statistical test described below can be found in Supplementary Table 1.

Shapiro–Wilk test was used to test for normality of the variables. For variables that were indistinguishable from normal distribution, parametric tests such as *t*-test, paired *t*-test, ANOVA, and mixed ANOVAs were used. For data that were distinguishable from normal distribution, nonparametric tests such as Kruskal–Wallis test, Spearman's rank correlation, and Wilcoxon rank sum test were used. Multiple comparison was adjusted for using the Holm's method, Tukey's honest significance difference (HSD), or Benjamini-Hochberg method as appropriate. Outliers were removed from analysis if they have corresponding lab notes indicating a technical problem while collecting the data (technical outliers).

Microbiome beta diversity metrics were analyzed using permutational analysis of variance (PERMANOVA)[63] with R package vegan (v2.6.4).[62] For each sample type, microbial taxa were aggregated at phylogenetic ranks genus and above and only taxa with at least 10 reads in 20% or more samples were included for differential abundance and correlation analysis. For lung tissue taxa, differential abundance analysis considered the following variables: intranasal treatment and diet for mice that did not undergo surgery; and intranasal treatment and surgery for mice fed HFD. For fecal taxa, differential abundance analysis considered the following variables: diet, genotype, and timepoint for mice that did not receive surgery; and surgery, genotype, and timepoint for mice fed HFD. At each taxonomic rank, taxa were identified as differentially abundant with Analysis of Compositions of Microbiomes II (ANCOM II) using package *ANCOMBC* (v2.2.0)[64] and Differential Expression analysis for Sequence count data 2 (DESeq2) using package *DESeq2* (v1.40.2).[65] Only taxa that were identified as differentially abundant by both tools (Holm-corrected $p < 0.05$ for both) were considered significant. The relative abundance of these differentially abundant taxa was then used to test for correlations with select host data (body weight, glucose tolerance metrics, serum metabolic markers excluding insulin, percentages of BALF eosinophils and neutrophils, lung histology scores and lung peribronchial trichrome area) using Spearman's rank test with Benjamini–Hochberg (BH) correction.

Data and Code Availability

Sequencing data is deposited in Sequencing Read Archive (SRA) under BioProject ID PRJNA1111477. Code for data processing and analysis is publicly available on https://github.com/yk132/GLP_KO_Microbiome_final. The computing environment for data processing and analysis is available at https://gitlab.oit.duke.edu/mic-course/2023-mic-singularity-image.

Results

High Fat Diet Led to Weight Gain, Glucose Intolerance, and Metabolic Imbalance

In mice that did not undergo surgery (total n = 57), a mixed ANOVA of mice body weight on timepoint (ie, weeks 0, 10, and 13), sex, diet and genotype identified significant three-way interaction effect between timepoint (ie, weeks 0, 10, and 13), sex, and diet ($p < 1E-6$), but none of the effects involving genotype was significant. Specifically, mice fed on a high fat diet weighed significantly more than mice fed on normal chow on weeks 10 and 13 (*t*-test, Holm-adjusted $p < 0.05$, Figure 2A). While all mice gained weight in the first 10 weeks of experiment (Tukey's HSD, $p < 0.0001$) as well as the overall duration of the experiment (ie, week 0 to 13; Tukey's HSD, $p < 0.0001$), a sex effect was observed in only mice fed HFD. Male mice fed HFD gained significantly more weight as compared to female counterparts between weeks 0 and 10 (paired *t*-test, Holm-adjusted $p < 0.05$) and between weeks 0 and 13 (paired *t*-test, Holm adjusted $p < 0.05$).

In this cohort of mice that did not undergo surgery, three glucose tolerance metrics (area under the curve [AUC], baseline glucose, and peak glucose level) were measured from 41 mice. Mixed ANOVA on each of these glucose tolerance metrics on diet, sex, timepoint, and genotype showed significant two-way interaction between diet and timepoint for all metrics and significant sex effect on baseline glucose only (Holm-adjusted $p < 0.01$). However, as with body weight, none of the effects involving genotype was significant. The effect of sex was significant and was only significant for baseline glucose (mixed ANOVA, Holm-adjusted $p < 0.05$). Mice-fed HFD displayed significantly more

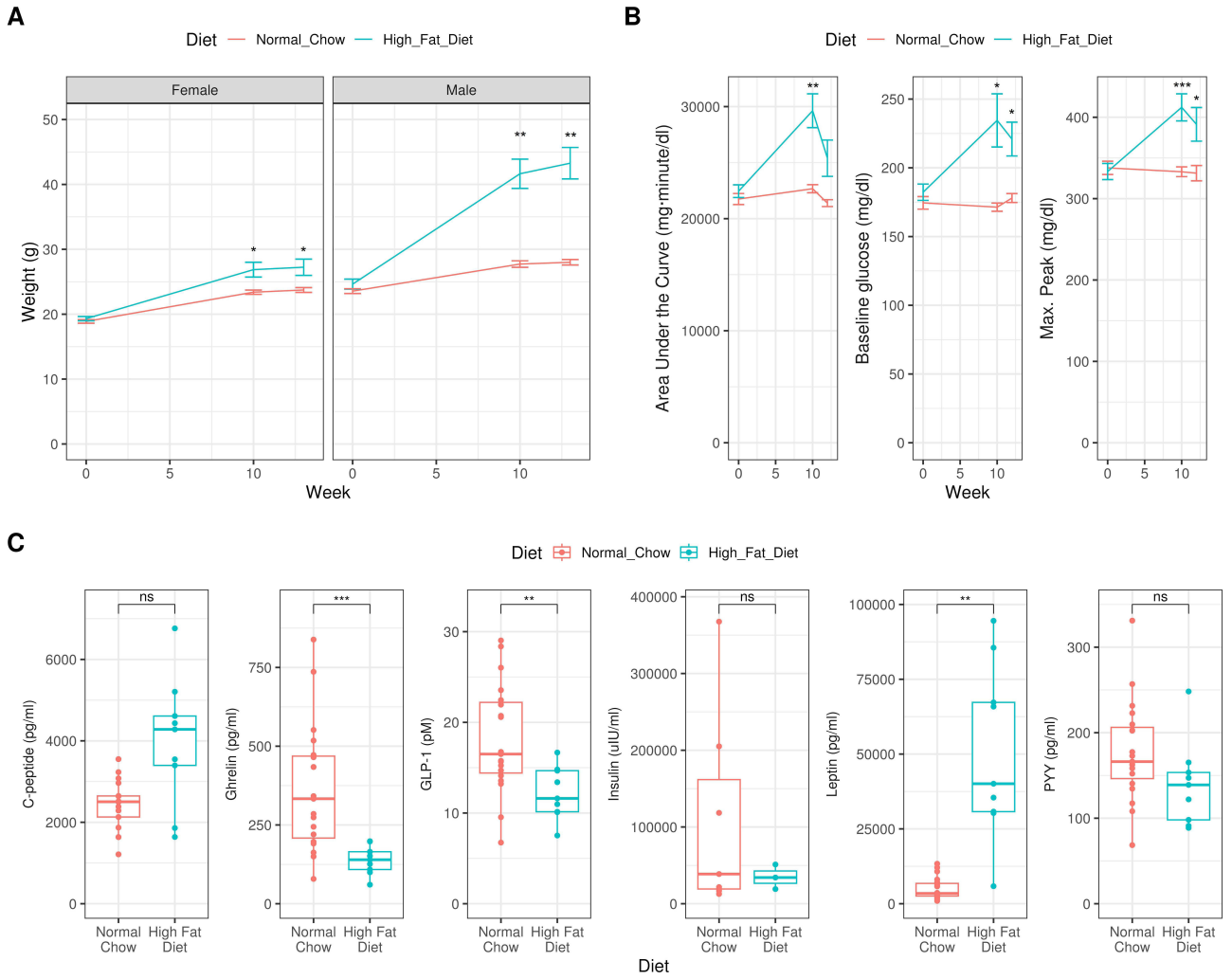

Figure 2 High fat diet leads to body weight gain, glucose intolerance, and changes in levels of serum metabolic markers. (**A**) In mice that did not receive surgery, high fat diet led to significant body weight gain (n = 8-16 per group) and (**B**) glucose intolerance over time (n = 9-18 per group) compared to mice fed normal chow. Data are shown as mean ± standard error in A and B. (**C**) In this cohort, changes in serum metabolic markers were observed at week 13 based on diet (C; n = 4-10 per group). Significance is based on *t*-tests. Not significant (ns), $p > 0.05$; *$p < 0.05$; **$p \leq 0.01$; ***$p \leq 0.001$.

glucose intolerance compared to mice fed normal chow in week 10, as denoted by significantly higher AUC, baseline glucose, and peak glucose levels (*t*-test, Holm-adjusted $p < 0.05$; Figure 2B). We note that all mice received a 1 week break from being fed a high-fat diet after week 10 regardless of surgery status, which explains the reduced glucose intolerance in week 12 on mice fed HFD (Figure 2B). In these mice fed HFD that did not undergo surgery, male mice had significantly higher baseline glucose levels compared to female counterparts in week 12 (*t*-test, Holm-adjusted $p < 0.05$) but not in other weeks.

Six serum metabolic markers, namely C-peptide, leptin, ghrelin, GLP-1, insulin, and Peptide YY (PYY) were measured from a total of 28 mice that did not undergo surgery. ANOVA of each serum metabolic marker, except for insulin due to low n, on sex and diet identified significant effect of diet on serum levels of C-peptide, ghrelin, and leptin (Holm-adjusted $p < 0.01$) and significant two-way interaction between sex and diet for leptin (Holm-adjusted $p < 0.0001$). Specifically, mice fed HFD had significantly higher serum levels of leptin (*t*-test, Holm-adjusted $p < 0.01$) but significantly lower levels of ghrelin (Holm-adjusted *t*-test, $p < 0.001$) and GLP-1 (*t*-test, Holm-adjusted $p < 0.01$) as compared to mice fed normal chow (Figure 2C). Furthermore, male mice had significantly higher circulating leptin levels than female mice for both diets (*t*-test, Holm-adjusted $p < 0.01$ for both; Supplementary Figure 1). As depicted in

https://doi.org/10.2147/JAA.S478329

Figure 2C, no significant differences based on diet were observed in serum levels of C-peptide (*t*-test, Holm-adjusted $p = 0.06$), insulin (*t*-test, Holm-adjusted $p = 0.2$) or PYY (*t*-test, Holm-adjusted $p = 0.2$).

Vertical Sleeve Gastrectomy Remediated Effects of High Fat Diet on Weight and Glucose Intolerance

After establishing that high fat diet led to expected results of weight gain (Figure 2A), glucose intolerance (Figure 2B), and metabolic imbalance (Figure 2C), we focused on mice fed HFD to test for the effect of surgery. These mice underwent either VSG, sham surgery, or no surgery (control) in week 10 (n = 55). In this HFD-fed cohort, mixed ANOVA of body weight on timepoint (pre-surgery week 10 and post-surgery week 13), surgery status, sex, and genotype identified significant three-way interaction between surgery, sex, and timepoint (pre-surgery week 10 and post-surgery week 13, $p < 0.01$), but no effects involving genotype were significant. Specifically, male mice that underwent VSG lost significantly more body weight following surgery compared to male mice that underwent sham surgery or no surgery (Figure 3A; Tukey's HSD, $p < 0.05$ for all). These significant differences were not observed in female mice (Figure 3A; Tukey's HSD, $p \geq 0.08$).

In addition to reductions in body weight, mice that received VSG exhibited significantly reduced glucose intolerance post-operative (week 12) as compared to mice that did not receive any surgery. This difference was marked by significantly lower baseline glucose, max. glucose peak, and area under the curve compared to mice that did not undergo any surgery (Figure 3B; Tukey's HSD, $p < 0.05$). However, significant differences in glucose tolerance metrics were not detected between no surgery and sham surgery groups, or between sham surgery and VSG surgery groups (Figure 3B; Tukey's HSD, $p \geq 0.07$). Insufficient serum metabolic marker measurements in this cohort precluded testing for the effect of VSG. The circulating levels of metabolic markers did not differ significantly between sham surgery and no surgery groups (*t*-test, Holm-adjusted $p \geq 0.06$), nor did they differ based or genotype (*t*-test, Holm-adjusted $p \geq 0.07$).

Allergic Airway Inflammation was Induced by Intranasal Treatment of HDM Allergen

A subgroup of mice underwent BALF collection for differential immune cell counting and histology of lung sections with H&E, PAS, and Masson's trichrome stains to test for the effects of intranasal treatment with HDM allergen on respiratory inflammation as compared to treatment with PBS (n = 21 for PBS, 22 for HDM). Mice that were intranasally instilled with HDM allergen had significantly higher relative proportions of eosinophils and neutrophils in BALF compared to mice treated with PBS (Figure 4A, Wilcoxon test, Holm-adjusted $p < 0.0001$). We also observed a corresponding lower percentage of macrophages and epithelial cells in BALF of HDM-treated mice compared to PBS-treated mice (Figure 4A, Wilcoxon test, Holm-adjusted $p < 0.0001$).

Furthermore, peribronchial H&E staining and airway PAS staining scores were both significantly elevated in HDM-treated mice as compared to mice treated with PBS (Figure 4B, *t*-test, $p < 1E\text{-}6$). In addition, the average percentage of peribronchial Masson's trichrome stained area was higher in HDM-treated mice (Figure 4C, *t*-test, $p = 0.001$). Representative images of lung histology, presented in Figure 4D, support these findings by demonstrating that HDM-challenged mice have increased peribronchial inflammation (H&E stain), excessive airway mucus production (PAS stain), and increased peribronchial collagen deposition, indicative of airway fibrosis (Masson's trichrome stain), as compared to control (PBS)-challenged mice.

Neither Intranasal Treatment nor HFD Appreciably Altered Murine Lung Tissue Microbiome

As expected, visually inspecting microbial composition in each sample type at phylum level displayed differences in microbiome composition between fecal and lung tissue samples (Figure 5). The fecal microbiome was dominated by phyla Firmicutes, Bacteroidota (formerly Bacteroidetes), and Actinobacteria. In comparison, the lung microbiome was dominated by phyla Proteobacteria, Actinobacteria, and Bacteroidota, with some samples displaying high Firmicutes prevalence.

While 48 murine lung tissue samples were collected, 2 of the samples were not sequenced due to human error and 2 samples were removed from analysis due to low number of sequencing reads, leading to a total of 44 lung tissue microbiome samples included in analysis. As is standard in the analysis of multi-dimensional microbiome data, we

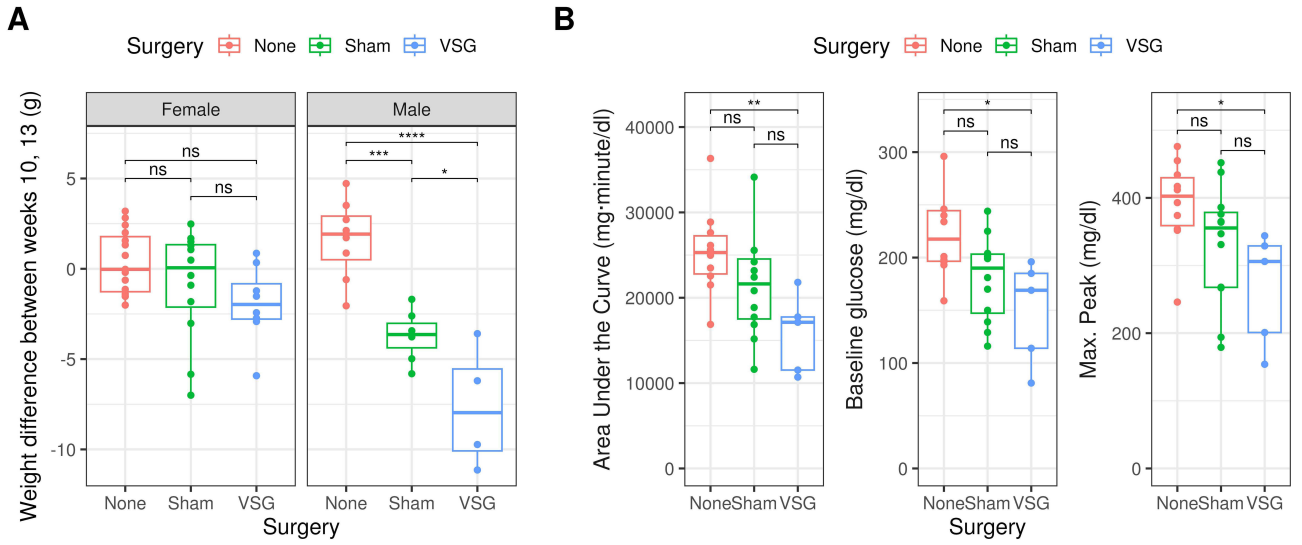

Figure 3 Bariatric surgery remediates weight gain and glucose intolerance metrics in mice fed HFD. (**A**) Between pre- and post-surgery timepoints, male mice lost increasingly more weight from no surgery group, sham surgery group, to VSG group. These differences were not significant in female mice (Tukey's HSD test, n = 4-15 per group). (**B**) Glucose tolerance metrics at post-surgery timepoint were lower in mice that underwent VSG compared to mice that did not undergo any surgery (Tukey's HSD test, n = 5-12 per group). Not significant (ns), $p > 0.05$; *$p < 0.05$; **$p \leq 0.01$; ***$p \leq 0.001$; ****$p \leq 0.0001$.

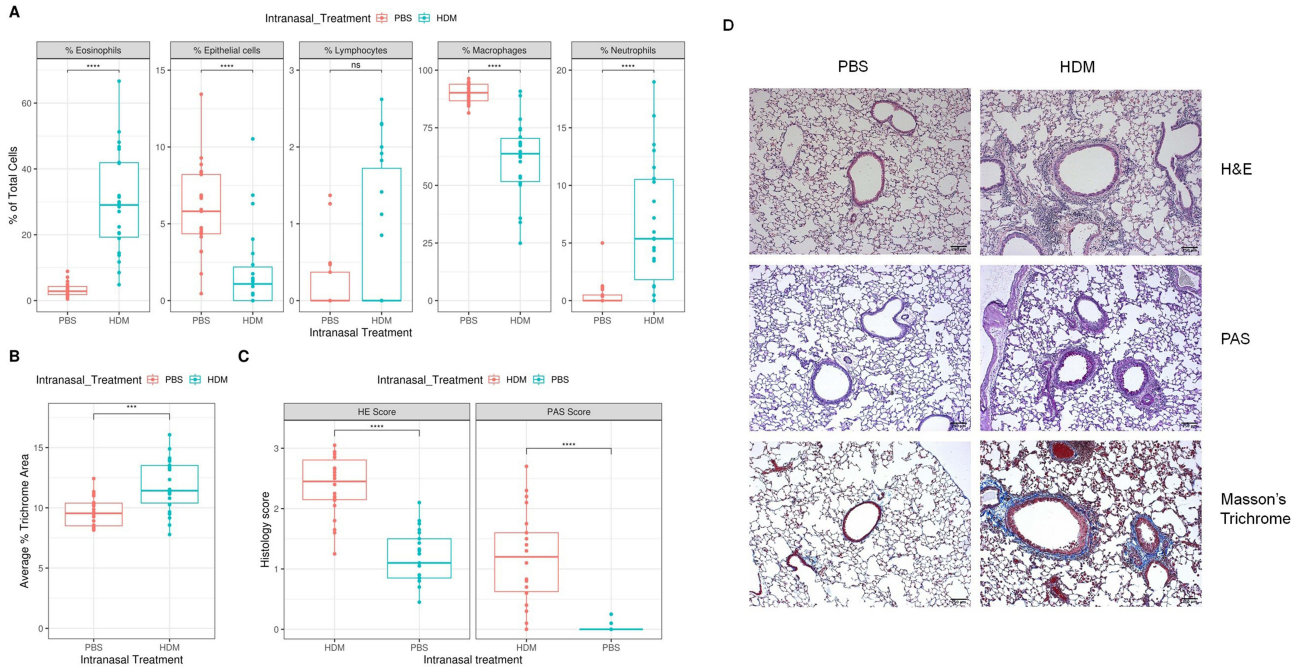

Figure 4 Intranasal exposure of HDM allergen induced airway inflammation and fibrosis. (**A**) Percentage of each immune cell type from BALF of mice sacrificed on week 13, (**B**) percent peribronchial Masson's trichrome-stained area and (**C**) average peribronchial H&E and PAS scores in each mouse from 10 airway sections are presented by intranasal treatment (n = 21 for PBS, 22 for HDM). (**D**) Representative images at 20x magnification of lung sections from PBS- or HDM-challenged mice stained with H&E, PAS or Masson's trichrome stains. Significance is based on Holm-corrected Wilcoxon rank sum test (**A**) or *t*-test (**B** and **C**). Not significant (ns), $p > 0.05$; ***$p \leq 0.001$; ****$p \leq 0.0001$.

compared the alpha diversity, ie the within-community diversity of the microbial samples. Herein, we used three alpha diversity metrics: observed richness, Shannon diversity index, and Faith's phylogenetic diversity (PD). Observed richness refers to the species richness within the sample, whereas Shannon diversity incorporates both richness and evenness,[57] and Faith's PD uses a phylogenetic tree to account for the evolutionary diversity within a sample.[58] Analyzing the alpha diversity metrics of lung tissue microbiome in mice that did not undergo any surgery (n = 26) did not reveal significant

https://doi.org/10.2147/JAA.S478329

Figure 5 Relative abundance of all microbiome samples at phylum level based on sample type. Fecal microbiome data are from 177 samples across 3 timepoints (n = 89) and lung tissue microbiome data are from 44 samples from 2 timepoints (n = 44). Fecal microbiome samples are ordered by prevalence of Firmicutes whereas lung tissue samples are ordered by prevalence of Proteobacteria.

differences based on intranasal treatment, genotype, or timepoint (mixed ANOVA; Holm-adjusted $p = 1.0$). Similarly, for mice fed HFD (n = 23), no significant effect of intranasal treatment, surgery, or their interaction terms was detected for any of the lung tissue microbiome alpha diversity metrics (mixed ANOVA, Holm-adjusted $p \geq 0.6$).

We then analyzed the beta diversity of the microbiome data, which measures the degree of dissimilarity in microbiome composition between samples. We adopted two beta diversity metrics: UniFrac distance is based on phylogenetic distance between the observed bacterial taxa, while weighted UniFrac distance leverages both phylogenetic distance and relative abundance of the taxa.[66] For mice that did not undergo any surgery (n = 26), PERMANOVA of UniFrac and weighted UniFrac metrics did not detect significant changes in lung tissue microbiome composition based on genotype or intranasal treatment ($p > 0.3$ for both). In parallel, for mice fed high fat diet (n = 23), PERMANOVA of neither UniFrac nor weighted UniFrac metrics revealed significant shifts in lung tissue microbiome composition based on surgery status ($p > 0.3$ for both).

Lastly, we tested whether bacteria hat were more prevalent in one group than another based on variables of interest existed. No bacterial taxa in lung tissue samples were identified as being differentially abundant based on intranasal treatment and diet in mice that did not undergo any surgery (n = 26, ANCOM II and DESeq2, Holm-adjusted $p > 0.05$ for one or both). Similarly, for mice that were fed HFD (n = 23), no bacterial taxa were identified as being differentially abundant based on intranasal treatment and surgery status (ANCOM II and DESeq2, Holm-adjusted $p > 0.05$ for one or both).

High Fat Diet Reduces Prevalence of SCFA-Producing Bacteria in Fecal Microbiome

We collected a total of 117 fecal pellets from 58 mice that did not undergo surgery. We conducted ANOVA for each alpha diversity metric, assessing the effects of diet, timepoint, and genotype. None of the main effects or interactions approached the significance threshold of 0.05 (Holm-adjusted $p > 0.54$), except for the interaction between diet and timepoint on Faith's PD (Holm-adjusted $p = 0.11$). This suggestive trend is presented in Figure 6A, which shows that mice fed on a high fat diet had less diverse fecal microbiomes than their counterparts fed normal chow in later weeks.

UniFrac and weighted UniFrac beta diversity metrics were used to compare the fecal microbiome composition between groups of samples. In mice that did not receive any surgery (n = 58, 120 fecal pellets across 3 time points), PERMANOVA of both beta diversity metrics on diet, genotype, and timepoint revealed significant main effects of diet, genotype, and timepoint ($p < 0.01$ for all). Furthermore, two-way interaction between diet and sampling timepoint was

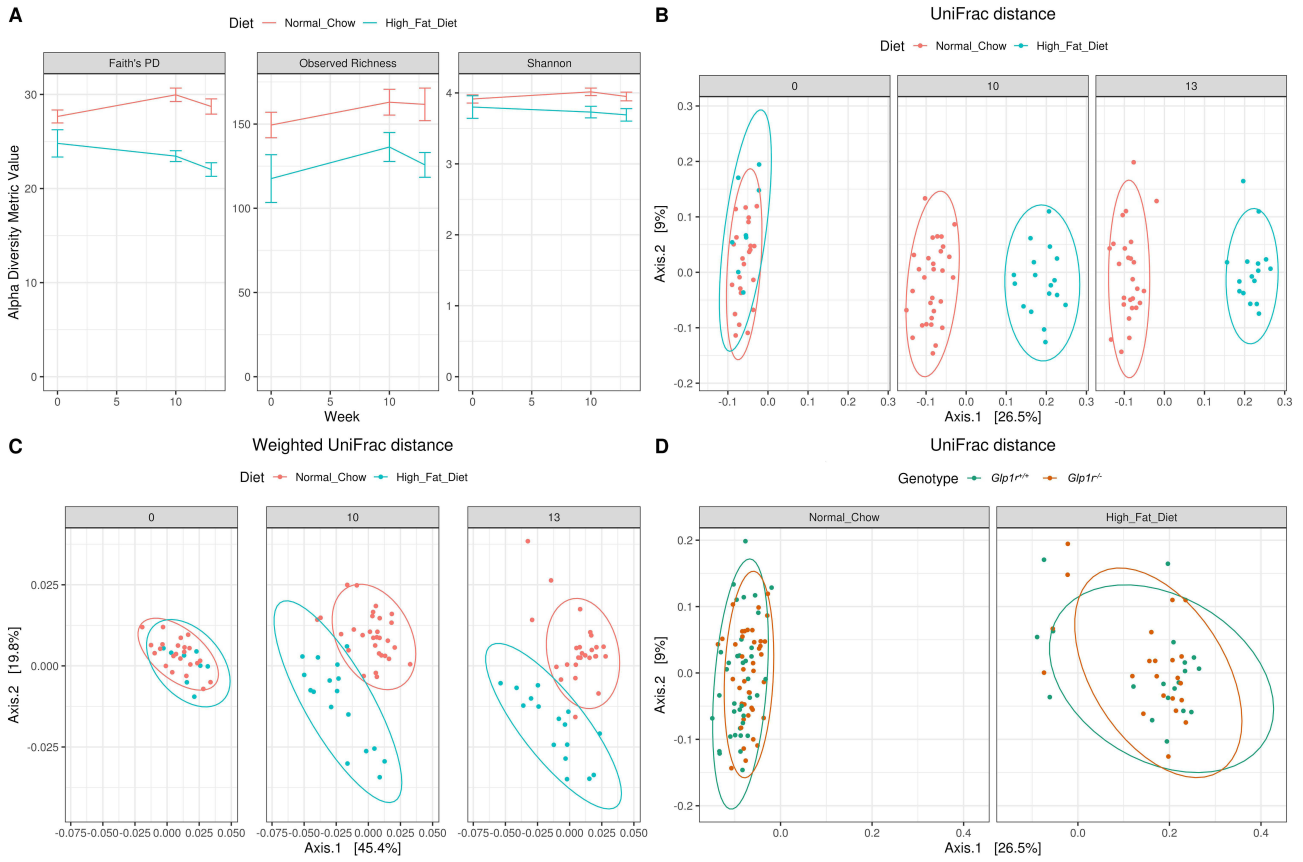

Figure 6 In mice that did not undergo surgery, fecal microbiome composition of mice fed HFD differed significantly from their normal chow-fed counterparts. (**A**) Alpha diversity metrics for fecal microbiome at weeks 0, 10, and 13 are shown by diet as mean ± standard error (n = 8-30 per group at each timepoint). Throughout the experiment, both (**B**) UniFrac and (**C**) weighted UniFrac distances displayed clustering by diet in later weeks (PERMANOVA, $p<0.0001$, n = 8-30 per group at each timepoint). (**D**) The two-way interaction between genotype and diet was significant for UniFrac distance in this cohort (PERMANOVA, $p < 0.05$, n = 19-41 per group). Data are shown as principal coordinate plots with 95% confidence ellipses (**B**–**D**).

highly significant for both UniFrac and weighted UniFrac metrics, indicating that diet led to differential changes in fecal microbiome composition over time (Figure 6B and C; PERMANOVA, $p = 0.0001$). Significant two-way interaction between diet and genotype was observed only for UniFrac distance (Figure 6D; PERMANOVA, $p < 0.05$).

Since beta diversity analysis with UniFrac and weighted UniFrac distances detected significant differences in fecal microbial composition based on diet, we tested which bacterial taxa were driving these differences. In mice that did not receive surgery, the prevalence of 41 fecal taxa significantly differed by diet and sampling timepoint (weeks 0, 10, or 13; n = 58, ANCOM II and DESeq2, Holm-adjusted $p < 0.05$ for both tests). A total of 11 taxa were more abundant in fecal microbiome of mice fed HFD, whereas 30 other taxa were more abundant in that of mice fed normal chow. The identities of these taxa and their differential abundance based on diet are summarized in Table 1. Of these 40 taxa, 5 taxa were also identified as being differentially abundant by genotype in addition to diet: *Prevotellaceae UCG-001, Romboutsia, Candidatus Arthromitus*, Peptostreptococcaceae, and Peptostreptococcales-Tissierellales (n = 58, ANCOM II and DESeq2, Holm-adjusted $p < 0.05$ for both). However, relative abundance of each of these taxa did not differ significantly between *Glp1r*-replete and -deficient mice when tested within each diet and timepoint (Wilcoxon rank sum test, Holm-adjusted $p > 0.4$).

To further understand how these diet-associated fecal bacterial taxa may be associated with host health, the prevalence of each significant differentially abundant taxon was correlated with select host metadata as described in methods. All 246 significant correlations are reported in Supplementary Table 2 (n = 34–90, Spearman's rank correlations, BH-adjusted $p < 0.05$). Of these myriad results, we highlight three fecal microbiome taxa linked to short chain fatty acid production and thus, potentially, the gut-lung microbiome axis: *Lachnospiraceae UCG-001, Bifidobacterium*, and *Parasutterella*. In mice that did not undergo surgery, the prevalence of these three taxa in

Table 1 List of Differentially Abundant Taxa in Fecal Samples Based on Diet for Mice That Did Not Undergo Surgery

Phylogenetic Rank	Higher Prevalence in Fecal Microbiome at Weeks 10 and 13	
	Mice Fed Normal Chow	**Mice Fed High Fat Diet**
Phylum	Actinobacteriota, Proteobacteria, Verrucomicrobiota	
Class	Actinobacteria, Coriobacteriia, Gammaproteobacteria, Verrucomicrobiae	
Order	Bifidobacteriales, Burkholderiales, Coriobacteriales, Clostridia UCG-014	Oscillospirales, Peptostreptococcales-Tissierellales
Family	*[Eubacterium] coprostanoligenes group, Anaerovoracaceae, Atopobiaceae, Bifidobacteriaceae, Lactobacillaceae, Muribaculaceae, Prevotellaceae, Sutterellaceae*	*Enterococcaceae, Peptostreptococcaceae, Streptococcaceae*
Genus	*Bifidobacterium, Butyricicoccus, Candidatus Arthromitus, Coriobacteriaceae UCG-002, HT002, Lachnospiraceae UCG-001, Muribaculum, Parasutterella, Prevotellaceae NK3B31 group, Prevotellaceae UCG-001, Tyzzerella*	*Acetatifactor, Lactococcus, Rikenella, Rikenellaceae RC9 gut group, Romboutsia, Tuzzerella*

Notes: A list of fecal taxa that were identified as differentially abundant based on diet in mice that did not undergo surgery. The columns indicate whether the prevalence of each taxon was higher in mice fed normal chow or a high fat diet in weeks 10 and 13 (DESeq and ANCOM II, Holm-adjusted $p < 0.05$ for both, n = 58).

fecal microbiome was significantly reduced in mice fed HFD compared to their counterparts fed normal chow by weeks 10 and 13 (Figure 7A, C, E; n = 58, ANCOM II and DESeq2, Holm-adjusted $p< 0.05$ for both). Furthermore, the relative abundance of each of these three taxa was positively correlated with circulating GLP-1 levels at sacrifice (Figure 7B, D, F; n = 38, Spearman's rank correlations, BH-adjusted $p < 0.05$) and negatively correlated with all three glucose tolerance metrics and body weight (Supplementary Table 2; n = 58 and 90, respectively, Spearman's rank correlation, BH-corrected $p < 0.05$).

Bariatric Surgery Has Limited Effect on Fecal Microbiome at 3 weeks After Surgery

To evaluate the effect of VSG surgery, sham surgery, or no surgery (control) on fecal microbiome composition, we focused on the post-surgery timepoint of week 13 in mice fed HFD (n = 45). For these mice, ANOVA of each alpha diversity metric on surgery, genotype, and sex did not reveal any significant main effect or interaction terms (Supplementary Figure 2; Holm-adjusted $p = 1.0$). Furthermore, PERMANOVA of beta diversity metrics on surgery status and genotype did not detect appreciable effect of surgery ($p > 0.08$, n = 12–17 per group) or its interaction with genotype ($p > 0.43$) on fecal microbiome composition. In comparison, significant differences were observed in fecal microbiome composition between $Glp1r^{-/-}$ and $Glp1r^{+/+}$ genotypes for this cohort (Figure 8; PERMANOVA, $p < 0.05$ for both metrics). No fecal taxa were identified as being differentially abundant based on surgery status and genotype at post-surgery timepoint of week 13 for these mice fed HFD (n = 45, ANCOM II and DESeq2, Holm-adjusted $p > 0.05$ for one or both tests).

To summarize all the presented results, in Table 2 we gathered the significant findings from all statistical tests performed. Details on statistical tests are available in Supplementary Table 2 and code for analysis is publicly available as a Git repository (https://github.com/yk132/GLP_KO_Microbiome_final).

Discussion

The complex influences of obesity on asthma pathobiology have become increasingly recognized by researchers and clinicians. Mouse models that approximate disease mechanisms in humans are essential tools in making progress to identify potential therapeutic targets in asthma. Our study utilized a model of diet-induced obesity paired with concurrent allergic sensitization and challenge, followed by metabolic surgery to investigate mechanisms of obesity-associated allergic airways disease with bariatric surgery. As expected, feeding mice on a high fat diet led to increased body weight and glucose intolerance compared to mice fed normal chow (Figure 2A and B). Furthermore, HFD-fed mice exhibited metabolic imbalance such as reduced circulating GLP-1 and ghrelin levels, whereas serum leptin levels were elevated compared to normal chow-fed mice (Figure 2C). Being on a HFD also altered the fecal microbiome: fecal microbiome of

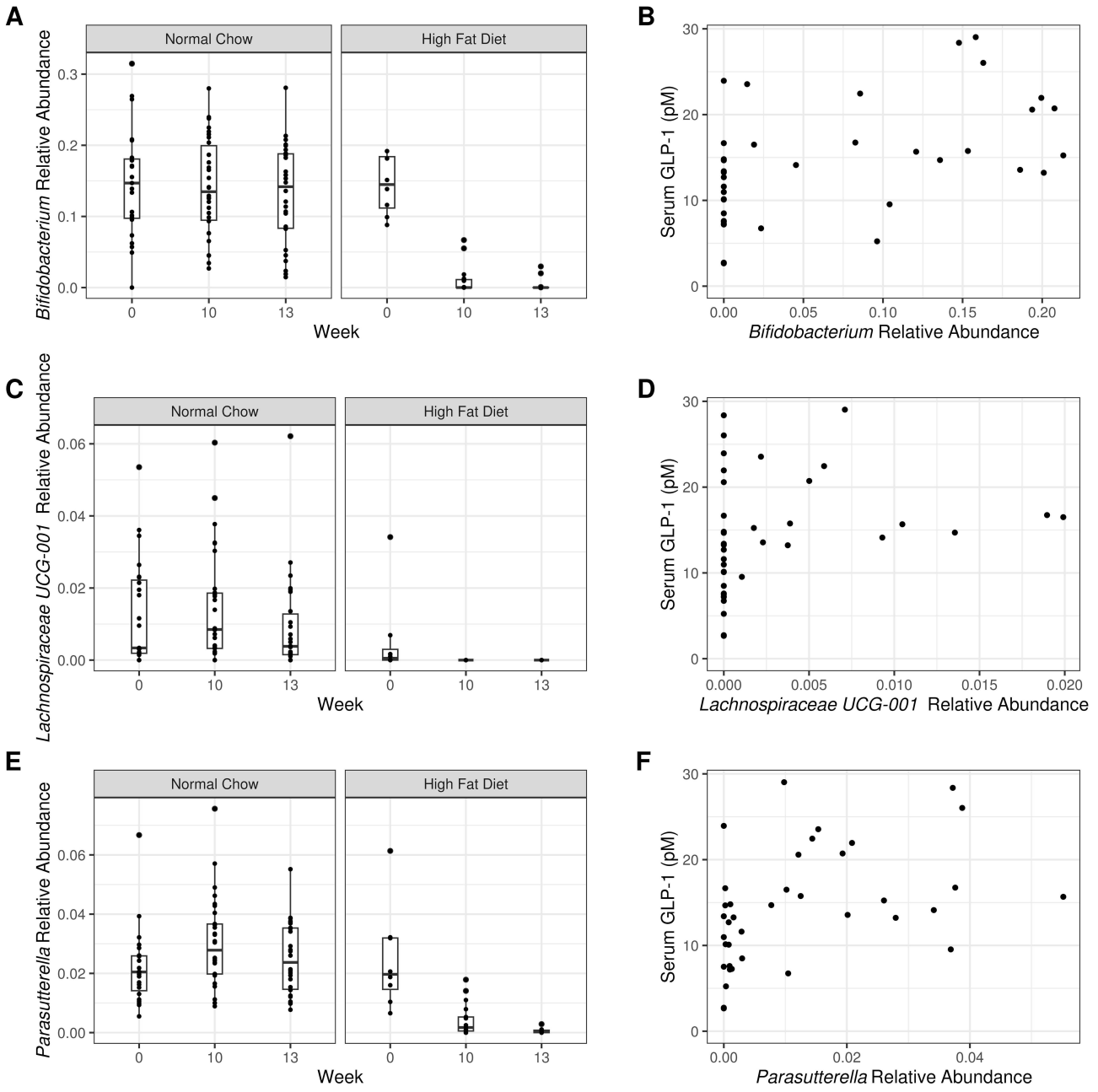

Figure 7 Prevalence of fecal taxa associated with short chain fatty acid production were reduced in mice fed high fat diet. The relative abundance of (**A**) *Bifidobacterium*, (**C**) *Lachnospiraceae* UCG-001, and (**E**) *Parasutterella* were significantly lower in fecal samples of high fat diet-fed mice on weeks 10 and 13 (ANCOM II and DESeq2, Holm-adjusted $p<0.05$ for both, n = 4-15 per group). (**B, D, F**) At sacrifice, the relative abundance of these taxa was positively correlated with circulating GLP-1 levels (Spearman's rank correlation, BH-adjusted $p < 0.05$, n = 38).

mice fed HFD was significantly less diverse than that of mice fed normal chow by week 10 based on all three alpha diversity metrics used (Figure 6A). Based on beta diversity analysis, the composition of fecal microbiome changed based on diet over time (Figure 7B and C).

These results support that the diet-induced obesity model produced expected results. The increased serum leptin levels and decreased GLP-1 and ghrelin levels (Figure 2C) have been reported in humans with obesity, suggesting that the HFD model successfully induced metabolic imbalance similar to that observed in humans.[67–71] The extensive impact of diet, including high fat diet, on the gut microbiome has been well-documented.[72,73] For instance, increased fat content in diet, specifically fat and saturated fatty acids, is associated with lower diversity of gut microbiota,[74] as was observed herein.

https://doi.org/10.2147/JAA.S478329

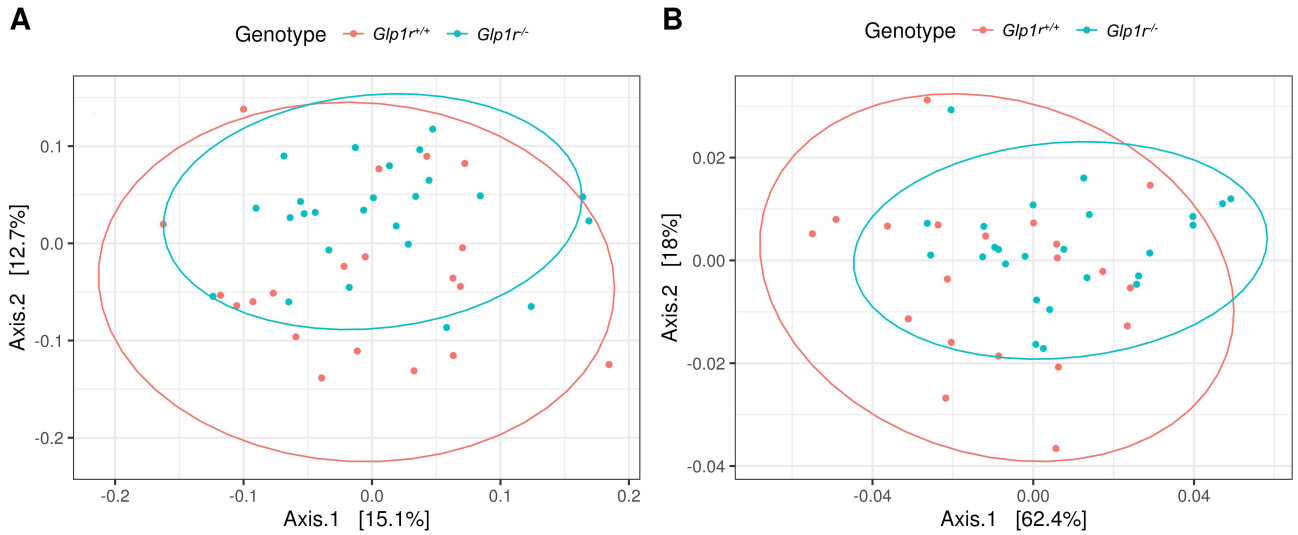

Figure 8 Fecal microbiome beta diversity metrics differed significantly by genotype for mice fed HFD on week 13. Both (**A**) UniFrac and (**B**) weighted UniFrac distances clustered significantly based on genotype (*Glp1r*$^{+/+}$, n = 20 and *Glp1r*$^{-/-}$, n = 25; PERMANOVA, $p < 0.05$ for both). Data are shown as PCoA plots with 95% confidence ellipses.

In addition to the diet-induced obesity model, intranasal treatment with HDM led to allergic airway disease and fibrosis as intended. In mice challenged with HDM, there was an influx of eosinophils and neutrophils in BALF (Figure 4A), increased peribronchial inflammation and collagen deposition, and excessive airway mucin production as compared to PBS-challenged mice (Figure 4B–D). Furthermore, these effects were observed across all mice from which

Table 2 Summary of Significant Experimental Results

Measurement	Models			
	High Fat Diet[a]	VSG Surgery[b]	House Dust Mite	*Glp1r*$^{-/-}$ genotype
Body weight	↑	↓ (male mice)	Not tested	–
Glucose tolerance	↓	↓ (VSG vs no surgery)	Not tested	–
Serum metabolic markers	Leptin ↑ Ghrelin, GLP-1 ↓	Not tested	Not tested	– (HFD group)
Airway inflammation and fibrosis	–	Not tested	H&E and PAS scores ↑ Eosinophils, neutrophils ↑ Trichrome stained area ↑	– (No surgery group; H&E and PAS scores)
Lung microbiome	–	–	–	–
Fecal microbiome	Δ UniFrac, Weighted UniFrac metrics Δ prevalence of 41 fecal taxa	–	Not tested	Δ UniFrac, weighted UniFrac metrics (No surgery group, HFD group)

Notes: Only significant experimental results are reported and groups within parentheses indicate sub-groups in which the results were valid. Δ denotes significant changes. [a]The effect of high fat diet were tested in mice that did not receive any surgery. [b]The effect of surgery status (no surgery, sham surgery, or VSG) was tested in mice fed on HFD.

Abbreviations: HFD, high fat diet; VSG, vertical sleeve gastrectomy; GLP-1, glucagon-like peptide-1; H&E, hematoxylin and eosin; PAS, Periodic acid-Schiff.

data were collected, regardless of surgery status, sex, genotype, or diet. These findings indicated the strong effects of intranasal HDM exposure on airway pathobiology.

After confirming that our model systems worked as intended, we specifically tested the hypothesis that a model of experimental bariatric surgery (VSG) will lead to increased GLP-1R signaling, resulting in improved allergen-induced airway inflammation through the modulation of the gut-lung microbiome axis. For these analyses, we focused on only mice fed on HFD, who underwent either no surgery, sham surgery, or VSG on week 10. VSG is a type of bariatric surgery that has gained worldwide popularity as it is minimally invasive when performed laparoscopically in humans.[75,76] In mice, however, VSG is performed via midline incision due to their small stomach size. As the stress of surgery could confound results, some mice underwent sham surgery, which was identical to VSG except for excision of the stomach. Thus, during sham surgery, the stomach was still separated, removed temporarily, and returned to the body cavity after briefly touching the stomach with a metal probe.[3]

In male mice, we observed significant increases in body weight loss from mice that received no surgery, sham surgery, to VSG (Figure 3A). A similar trend was observed in female mice, though not statistically significant (Figure 3A). Furthermore, we observed a significant reduction in glucose intolerance in VSG-operated mice compared to no surgery mice (Figure 3B), but not compared to sham-operated mice. Together, these data support that the body weight loss observed in VSG mice after surgery was not attributable to the stress of surgery alone, as male mice that underwent VSG lost significantly more weight than those that received sham surgery. Instead, the weight loss was likely in part attributable to metabolic changes such as improved glucose homeostasis. Indeed, improved metabolism, including restored glucose homeostasis, is often reported following bariatric surgery,[77,78] suggesting that our VSG model produced expected results. Unfortunately, we had insufficient mice to test the role of bariatric surgery in circulating GLP-1 levels, in part because some mice did not survive the surgery.

Herein we did not observe a significant effect of *Glp1r* deficiency on body weight, glucose tolerance, or markers of allergic airway disease (Table 2). These findings contrast with the popularity of GLP-1R agonist drugs as therapies for weight loss and diabetes and recent studies suggesting that GLP-1R agonists may confer protection against respiratory illnesses.[32,79–81] A possible explanation of this discrepancy is that the endogenous GLP-1R stimulation in our mice cohort may be of lower magnitude as compared to stimulation with synthetic GLP-1R agonists. Furthermore, the model herein targeted the GLP-1 receptor, which would impact GLP-1R signaling but not necessarily the production or circulation of GLP-1. Thus, future studies analyzing the effects of administering exogenous GLP-1 or GLP-1R agonists in our models are warranted.

Lastly, we tested how our model systems (high fat diet, house dust mite allergen, VSG surgery, and genotype) affected the gut and lung microbiomes (Table 2). Current literature supports sustained changes in gut microbiome after bariatric surgery and posits that it may contribute to observed improvements in metabolic health.[16] However, human studies have been limited by a lack of longitudinal data and limited metadata on confounding variables that also affect the gut microbiome. Oftentimes the gut and lung microbiomes are studied separately, though the microbiota in the gut and the lung can influence each other via microbe-microbe and host-microbe interactions.[82] Thus, despite the prevalence of obesity in people with asthma,[2] studies that examine both in the context of either human disease or murine models of obesity and asthma are rare.[22] To further complicate matters, GLP-1 has also been posited as a gut microbiome regulator, although the details of bidirectional communication between gut microbiota and L-cells are still being uncovered.[83]

In this study, we did not observe significant changes in lung microbiome based on surgery, intranasal treatment, diet, or genotype (summarized in Table 2). As such, whether lung microbiome changes occur after bariatric surgery and their potential impact on asthma remains a knowledge gap. In this study, mice were sacrificed within 3 weeks after surgery to sustain the effectiveness of HDM allergen challenge. Future studies should consider a simpler model without HDM sensitization and longer experimental duration after surgery that may better elucidate the potential effect of obesity and high fat diet on the lung microbiome. Any longitudinal respiratory microbiome data from people receiving bariatric surgery or GLP-1R agonists would also begin to fill a knowledge gap.

In contrast to the lung microbiome, we detected significant changes in fecal microbiome based on diet (Figure 6A–C) and genotype (Figures 6D and 8). As expected, the effect of diet on fecal microbiome was most noticeable, as elucidated by PCoA plots showing clear clustering of fecal microbiome composition based on diet over time in mice that did not

undergo surgery (Figure 6B and C). Although not statistically significant, fecal microbiome of mice fed on a HFD were less diverse compared to their counterparts on a normal chow based on all three alpha diversity metrics in later weeks (Figure 6A). While the main effect of genotype and its interaction with diet were significant for UniFrac distance in these mice (Figure 6D), PCoA plots did not reveal strong and obvious clustering. These plots thus suggest that while GLP-1R signaling may influence the fecal microbiome, its effect is more subtle than diet.

While these diversity metrics are useful in interpreting complicated microbiome data, finer tests are needed to understand which taxa are driving these changes and how they may affect host health. The strong effect of diet on gut microbiome was evident as 41 fecal taxa were identified as differentially abundant based on diet in mice that did not receive any surgery (Table 1). Interestingly, a lower prevalence of some SCFA-producing or related bacteria was observed in mice fed high fat diet (as compared to normal chow) in no surgery group. Short chain fatty acids are bacterial metabolites elaborated from gut bacterial action of starch and fiber fermentation. Mostly composed of acetate (C2), propionate (C3), and butyrate (C4), SCFAs have gained enormous attention in recent years due to their ability to modulate the immune and metabolic systems.[84,85] SCFAs interact with G-protein coupled receptors 41 and 43 (GPR41, GPR43) and are present in neurons, adipocytes, enteroendocrine cells, and immune cells. These receptors are implicated in modulating cytokines levels, GLP-1 production, and adipogenesis.[86] For instance, SCFAs have been linked with reduced levels of proinflammatory cytokines including interleukin (IL)-4, IL-5, IL-13, and IL-17A, increased levels of anti-inflammatory IL-10, and increased differentiation of regulatory T cells.[16] In murine models, SCFA administration conferred protection against ovalbumin and papain-induced lung inflammation.[87,88] However, the role of SCFAs in obesity is hotly contested, as it serves as an extra energy source contributing to obesity while simultaneously increasing production of satiety hormones.[16]

As such, based on literature, we highlighted three anaerobic gut genera related to SCFAs that were significantly lower in fecal microbiome of mice fed HFD: *Bifidobacterium, Lachnospiraceae UCG-001*, and *Parasutterella*.[89–91] The relative abundance of these taxa were positively correlated with circulating GLP-1 levels and negatively correlated with leptin, glucose intolerance metrics, and weight (Supplementary Table 2). Members of *Bifidobacterium* genus can produce acetate and lactate, and their prevalence is often inversely correlated with obesity.[92] Furthermore, *Bifidobacterium* strains are popular probiotics. Supplementation of *Bifidobacterium longum* APC1472 reduced fasting glucose levels in people with obesity,[93] while a murine model using intranasal instillation with HDM demonstrated that *Bifidobacterium breve* MRx0004 significantly reduced neutrophil and eosinophil infiltration in BALF.[94] Thus, the observed reduction of *Bifidobacterium* in mice fed HFD is supported by literature, though future efforts should utilize microbial culturing and shotgun sequencing to increase taxonomic resolution and to gain insight on its function.

Lachnospiraceae family are spore-forming bacteria that are commonly found in both human gut and soil and produce butyrate and acetate.[95,96] Per usual, gut *Lachnospiraceae* modulations of health change based on different species, and likely strains, but growing research suggests that *Lachnospiraceae* play an important role in metabolic syndrome, diabetes, and obesity.[96] Moreover, this family could serve as a target for modulating the built environment for microbiome health as they are common in soil. For instance, in a mouse model, McCumber et al[95] described that lung and gut microbiome changes from soil exposure were driven by *Lachnospiraceae* taxa. The genus *Lachnospiraceae UCG-001* detected herein is not well characterized, though in a rat model it was negatively associated with biomarkers of type 2 diabetes mellitus.[97] Furthermore, Lan et al[98] reported that prevalence of Lachnospiraceae genera, including *Lachnospiraceae UCG-001*, were positively correlated with high-density lipoprotein cholesterol in humans. These studies suggest that *Lachnospiraceae UCG-001* may be beneficial for the host, and thus, the decrease in *Lachnospiraceae UCG-001* observed in mice fed HFD warrants further investigation.

Finally, *Parasutterella* is a core member of both human and murine gut microbiota that produce succinate.[91] Although succinate is not a SCFA, it affects SCFA production via cross-feeding as succinate is an important substrate for propionate generation.[99] Although our study reports a loss of *Parasutterella* in mice fed HFD, this genus has been associated with obesity, type 2 diabetes mellitus, and irritable bowel syndrome in humans.[100,101] In a murine model of diet-induced obesity, mice that were prone to obesity had significantly higher levels of gut *Parasutterella* (compared to obesity-resistance mice), and its relative abundance was significantly correlated with metabolites associated with obesity

phenotype.[102] Thus, the higher *Parasutterella* abundance in fecal microbiome of mice fed normal chow in the current study was unexpected, and its function in obesity remains to be characterized.

VSG surgery had limited effects on fecal microbiome at 3 weeks post-operative. Neither alpha diversity nor beta diversity metrics differed significantly by surgery type or its interactions. In parallel with results from mice that did not undergo surgery, in this cohort the fecal microbiome between mice with *Glp1r*$^{-/-}$ or *Glp1r*$^{+/+}$ genotypes differed significantly based on both UniFrac and weighted UniFrac metrics. However, PCoA plots displayed considerable overlap between the two genotypes' confidence intervals (Figure 8), again suggesting that the effect of genotype may be subtle. This observation may, in part, be due to sacrificing mice within 3 weeks of surgery to preserve the impact of HDM-induced allergic airway disease, as gut microbiome changes following bariatric surgery in humans are often studied 3–12 months post-surgery.[103] Future studies should consider simpler experimental models with longer duration that allow characterization of post-surgery gut microbiome. However, in this pilot study, we chose this model with HDM sensitization to mimic the patient population that may benefit most from bariatric surgery.

Conclusion

To summarize, this study aimed to characterize the role of GLP-1 receptor and gut-lung microbiome axis after bariatric surgery in a murine obese asthma model. While our model for diet-induced obesity and HDM-induced allergic airway disease generally produced expected results, the complicated study design as well as low number of mice hindered analysis of the effect of surgery. Contrary to our hypothesis, *Glp1r*$^{-/-}$ genotype did not appreciably alter host health metrics, such as body weight, glucose tolerance, and markers of allergic airway disease. Fecal microbiome composition in mice with *Glp1r*$^{-/-}$ genotype differed significantly from their counterparts with *Glp1r*$^{+/+}$ genotype, suggesting that GLP-1R signaling may be a fecal microbiome regulator. However, the effect of genotype was limited compared to a high fat diet. Gut microbiome taxa of HFD-fed mice differed significantly from their normal chow-fed counterparts, including reduced prevalence of SCFA-associated taxa *Bifidobacterium, Lachnospiraceae UCG-001*, and *Parasutterella*. Future studies investigating both lung and gut microbiomes in human participant-matched samples could point to novel therapeutic targets for obesity-associated asthma endotypes.

Acknowledgments

The authors thank the Duke Microbiome Core for preparing amplicon libraries of lung tissue samples and the Duke University School of Medicine for the use of the Sequencing and Genomic Technologies Shared Resource, which provided sequencing services. We also thank Dr. Robert Dickson and Jennifer Baker for discussing lung tissue DNA extraction methods and IDEXX for performing histopathology.

Author Contributions

All authors made a significant contribution to the work reported, whether that is in the conception, study design, execution, acquisition of data, analysis and interpretation, or in all these areas; took part in drafting, revising or critically reviewing the article; gave final approval of the version to be published; have agreed on the journal to which the article has been submitted; and agree to be accountable for all aspects of the work.

Funding

This work was supported in part as appropriate by NIH/NHLBI 1R01HL130234 (JLI), Duke Microbiome Center Development Grant (JLI), and the Engineering Research Centers Program of the National Science Foundation under NSF Cooperative Agreement No. EEC-2133504 (CKG, YJK).

Disclosure

Dr Yeon Ji Kim reports grants from National Science Foundation, during the conduct of the study. Dr Jennifer Ingram reports grants from National Institutes of Health - National Heart, Lung and Blood Institute, grants from Duke University Microbiome Center Development Grant, during the conduct of the study; grants from Sanofi/Regeneron, outside the submitted work. The author(s) report no conflicts of interest in this work.

References

1. Moore WC, Meyers DA, Wenzel SE, et al. Identification of asthma phenotypes using cluster analysis in the severe asthma research program. *Am J Respir Crit Care Med*. 2010;181(4):315–323. doi:10.1164/rccm.200906-0896OC
2. Prevention CfDCa. Asthma and obesity. 2013. Available from: https://www.cdc.gov/asthma/asthma_stats/asthma_obesity.htm. Accessed June 18, 2021.
3. Womble JT, Ihrie MD, McQuade VL, et al. Vertical sleeve gastrectomy associates with airway hyperresponsiveness in a murine model of allergic airway disease and obesity. *Original Res Front Endocrinol*. 2023;14. doi:10.3389/fendo.2023.1092277
4. Wang E, Wechsler ME, Tran TN, et al. Characterization of severe asthma worldwide: data from the international severe asthma registry. *Chest*. 2020;157(4):790–804. doi:10.1016/j.chest.2019.10.053
5. Gibeon D, Batuwita K, Osmond M, et al. Obesity-associated severe asthma represents a distinct clinical phenotype: analysis of the British thoracic society difficult asthma registry patient cohort according to BMI. *Chest*. 2013;143(2):406–414. doi:10.1378/chest.12-0872
6. Dixon AE, Poynter ME. Mechanisms of asthma in obesity. pleiotropic aspects of obesity produce distinct asthma phenotypes. *Am J Respir Cell mol Biol*. 2016;54(5):601–608. doi:10.1165/rcmb.2016-0017PS
7. Kato H, Ueki S, Kamada R, et al. Leptin has a priming effect on eotaxin-induced human eosinophil chemotaxis. *Int Arch Allergy Immunol*. 2011;155(4):335–344. doi:10.1159/000321195
8. Kim HY, DeKruyff RH, Umetsu DT. The many paths to asthma: phenotype shaped by innate and adaptive immunity. *Nat Immunol*. 2010;11(7):577–584. doi:10.1038/ni.1892
9. Boulet L-P, Turcotte H, Martin J, Poirier P. Effect of bariatric surgery on airway response and lung function in obese subjects with asthma. *Respir Med*. 2012;106(5):651–660. doi:10.1016/j.rmed.2011.12.012
10. Dixon AE, Pratley RE, Forgione PM, et al. Effects of obesity and bariatric surgery on airway hyperresponsiveness, asthma control, and inflammation. *J Allergy Clin Immunol*. 2011;128(3):508–515.e2. doi:10.1016/j.jaci.2011.06.009
11. Reddy RC, Baptist AP, Fan Z, Carlin AM, Birkmeyer NJO. The effects of bariatric surgery on asthma severity. *Obes Surg*. 2011;21(2):200–206. doi:10.1007/s11695-010-0155-6
12. Guerron AD, Ortega CB, Lee H-J, Davalos G, Ingram J, Portenier D. Asthma medication usage is significantly reduced following bariatric surgery. *Surg Endosc*. 2019;33(6):1967–1975. doi:10.1007/s00464-018-6500-x
13. Hossain N, Arhi C, Borg C-M. Is bariatric surgery better than nonsurgical weight loss for improving asthma control? A systematic review. *Obes Surg*. 2021;31(4):1810–1832. doi:10.1007/s11695-021-05255-7
14. Xie L, Chandrasekhar A, DeSantis SM, Almandoz JP, de la Cruz-Muñoz N, Messiah SE. Discontinuation and reduction of asthma medications after metabolic and bariatric surgery: a systematic review and meta-analysis. *Obes Rev*. 2022;24(2):e13527. doi:10.1111/obr.13527
15. Dixon AE, Peters U. The effect of obesity on lung function. *Expert Rev Respir Med*. 2018;12(9):755–767. doi:10.1080/17476348.2018.1506331
16. Kim YJ, Womble JT, Gunsch CK, Ingram JL. The Gut/Lung microbiome axis in obesity, asthma, and bariatric surgery: a literature review. *Obesity*. 2021;29(4):636–644. doi:10.1002/oby.23107
17. Sankararaman S, Noriega K, Velayuthan S, Sferra T, Martindale R. Gut microbiome and its impact on obesity and obesity-related disorders. *Curr Gastroenterol Rep*. 2023;25(2):31–44. doi:10.1007/s11894-022-00859-0
18. Yao Y, Cai X, Fei W, Ye Y, Zhao M, Zheng C. The role of short-chain fatty acids in immunity, inflammation and metabolism. *Crit Rev Food Sci Nutr*. 2022;62(1):1–12. doi:10.1080/10408398.2020.1854675
19. Kim CH. Control of lymphocyte functions by gut microbiota-derived short-chain fatty acids. *Cell mol Immunol*. 2021;18(5):1161–1171. doi:10.1038/s41423-020-00625-0
20. Crovesy L, Masterson D, Rosado EL. Profile of the gut microbiota of adults with obesity: a systematic review. *Eur J Clin Nutr*. 2020;74(9):1251–1262. doi:10.1038/s41430-020-0607-6
21. Whiteside SA, McGinniss JE, Collman RG. The lung microbiome: progress and promise. *J Clin Invest*. 2021;131(15). doi:10.1172/JCI150473
22. Michalovich D, Rodriguez-Perez N, Smolinska S, et al. Obesity and disease severity magnify disturbed microbiome-immune interactions in asthma patients. *Nat Commun*. 2019;10(1):5711. doi:10.1038/s41467-019-13751-9
23. Galaris A, Fanidis D, Stylianaki E-A, et al. Obesity reshapes the microbial population structure along the gut-liver-lung axis in mice. *Biomedicines*. 2022;10(2):494. doi:10.3390/biomedicines10020494
24. Sanmiguel CP, Jacobs J, Gupta A, et al. Surgically induced changes in gut microbiome and hedonic eating as related to weight loss: preliminary findings in obese women undergoing bariatric surgery. *Psychosom Med*. 2017;79(8):880–887. doi:10.1097/PSY.0000000000000494
25. Ilhan ZE, DiBaise JK, Dautel SE, et al. Temporospatial shifts in the human gut microbiome and metabolome after gastric bypass surgery. *NPJ Biofilms Microbiomes*. 2020;6(1):12. doi:10.1038/s41522-020-0122-5
26. Palleja A, Kashani A, Allin KH, et al. Roux-en-Y gastric bypass surgery of morbidly obese patients induces swift and persistent changes of the individual gut microbiota. *Genome Med*. 2016;8(1):67. doi:10.1186/s13073-016-0312-1
27. Sánchez-Alcoholado L, Gutiérrez-Repiso C, Gómez-Pérez AM, García-Fuentes E, Tinahones FJ, Moreno-Indias I. Gut microbiota adaptation after weight loss by Roux-en-Y gastric bypass or sleeve gastrectomy bariatric surgeries. *Surg Obes Relat Dis*. 2019;15(11):1888–1895. doi:10.1016/j.soard.2019.08.551
28. Fouladi F, Brooks AE, Fodor AA, et al. The role of the gut microbiota in sustained weight loss following Roux-en-Y gastric bypass surgery. *Obes Surg*. 2019;29(4):1259–1267. doi:10.1007/s11695-018-03653-y
29. Tremaroli V, Karlsson F, Werling M, et al. Roux-en-Y gastric bypass and vertical banded gastroplasty induce long-term changes on the human gut microbiome contributing to fat mass regulation. *Cell Metab*. 2015;22(2):228–238. doi:10.1016/j.cmet.2015.07.009
30. Mabey JG, Chaston JM, Castro DG, Adams TD, Hunt SC, Davidson LE. Gut microbiota differs a decade after bariatric surgery relative to a nonsurgical comparison group. *Surg Obes Relat Dis*. 2020;16(9):1304–1311. doi:10.1016/j.soard.2020.04.006
31. Wang J-Y, Wang Q-W, Yang X-Y, et al. GLP− 1 receptor agonists for the treatment of obesity: role as a promising approach. *Front Endocrinol*. 2023;14:1085799. doi:10.3389/fendo.2023.1085799
32. Yu M, Wang R, Pei L, et al. The relationship between the use of GLP-1 receptor agonists and the incidence of respiratory illness: a meta-analysis of randomized controlled trials. *Diabetol Metab Syndr*. 2023;15(1):164. doi:10.1186/s13098-023-01118-6

33. Pang J, Feng JN, Ling W, Jin T. The anti-inflammatory feature of glucagon-like peptide-1 and its based diabetes drugs—Therapeutic potential exploration in lung injury. *Acta Pharmaceutica Sinica B*. 2022;12(11):4040–4055. doi:10.1016/j.apsb.2022.06.003
34. Xu J, Wei G, Wang J, et al. Glucagon-like peptide-1 receptor activation alleviates lipopolysaccharide-induced acute lung injury in mice via maintenance of endothelial barrier function. *Lab Invest*. 2019;99(4):577–587. doi:10.1038/s41374-018-0170-0
35. Toki S, Newcomb DC, Printz RL, et al. Glucagon-like peptide-1 receptor agonist inhibits aeroallergen-induced activation of ILC2 and neutrophilic airway inflammation in obese mice. *Allergy*. 2021;76(11):3433–3445. doi:10.1111/all.14879
36. Salehi M, D'Alessio DA. Effects of glucagon like peptide-1 to mediate glycemic effects of weight loss surgery. *Rev Endocr Metab Disord*. 2014;15(3):171–179. doi:10.1007/s11154-014-9291-y
37. Larraufie P, Roberts GP, McGavigan AK, et al. Important role of the GLP-1 axis for glucose homeostasis after bariatric surgery. *Cell Rep*. 2019;26(6):1399–1408.e6. doi:10.1016/j.celrep.2019.01.047
38. Garibay D, McGavigan AK, Lee SA, et al. β-cell glucagon-like peptide-1 receptor contributes to improved glucose tolerance after vertical sleeve gastrectomy. *Endocrinology*. 2016;157(9):3405–3409. doi:10.1210/en.2016-1302
39. Lutz TA, Bueter M. The use of rat and mouse models in bariatric surgery experiments. *Front Nutr*. 2016;3:25. doi:10.3389/fnut.2016.00025
40. Stevenson M, Lee J, Lau RG, Brathwaite CEM, Ragolia L. Surgical mouse models of vertical sleeve gastrectomy and Roux-en Y gastric bypass: a review. *Obes Surg*. 2019;29(12):4084–4094. doi:10.1007/s11695-019-04205-8
41. Martins T, Castro-Ribeiro C, Lemos S, et al. Murine models of obesity. *Obesities*. 2022;2(2):127–147. doi:10.3390/obesities2020012
42. Kong J, Yang F, Bai M, et al. Airway immune response in the mouse models of obesity-related asthma. *Front Physiol*. 2022;13:909209. doi:10.3389/fphys.2022.909209
43. Johnston RA, Theman TA, Lu FL, Terry RD, Williams ES, Shore SA. Diet-induced obesity causes innate airway hyperresponsiveness to methacholine and enhances ozone-induced pulmonary inflammation. *J Appl Physiol*. 2008;104(6):1727–1735. doi:10.1152/japplphysiol.00075.2008
44. Turnbaugh PJ, Bäckhed F, Fulton L, Gordon JI. Diet-induced obesity is linked to marked but reversible alterations in the mouse distal gut microbiome. *Cell Host Microbe*. 2008;3(4):213–223. doi:10.1016/j.chom.2008.02.015
45. Jahansouz C, Staley C, Bernlohr DA, Sadowsky MJ, Khoruts A, Ikramuddin S. Sleeve gastrectomy drives persistent shifts in the gut microbiome. *Surg Obes Relat Dis*. 2017;13(6):916–924. doi:10.1016/j.soard.2017.01.003
46. Haange S-B, Jehmlich N, Krügel U, et al. Gastric bypass surgery in a rat model alters the community structure and functional composition of the intestinal microbiota independently of weight loss. *Microbiome*. 2020;8(1):13. doi:10.1186/s40168-020-0788-1
47. Ihrie MD, McQuade VL, Womble JT, et al. Exogenous leptin enhances markers of airway fibrosis in a mouse model of chronic allergic airways disease. *Respir Res*. 2022;23(1):131. doi:10.1186/s12931-022-02048-z
48. Baker JM, Hinkle KJ, McDonald RA, et al. Whole lung tissue is the preferred sampling method for amplicon-based characterization of murine lung microbiota. *Microbiome*. 2021;9(1):99. doi:10.1186/s40168-021-01055-4
49. Mason KL, Erb Downward JR, Mason KD, et al. Candida albicans and bacterial microbiota interactions in the cecum during recolonization following broad-spectrum antibiotic therapy. *Infect Immun*. 2012;80(10):3371–3380. doi:10.1128/iai.00449-12
50. Caporaso JG, Ackermann G, Apprill A, et al. EMP 16S Illumina amplicon protocol. 2018. Available from: http://wwwearthmicrobiomeorg/protocols-and-standards/16s. Accessed February 14, 2025.
51. Illumina. 16S Metagenomic sequencing library preparation. Available from: https://emea.illumina.com/content/dam/illumina-support/documents/documentation/chemistry_documentation/16s/16s-metagenomic-library-prep-guide-15044223-b.pdf. Accessed March 01, 2024.
52. Callahan BJ, McMurdie PJ, Rosen MJ, Han AW, Johnson AJA, Holmes SP. DADA2: high-resolution sample inference from Illumina amplicon data. *Nature Methods*. 2016;13(7):581–583. doi:10.1038/nmeth.3869
53. Quast C, Pruesse E, Yilmaz P, et al. The SILVA ribosomal RNA gene database project: improved data processing and web-based tools. *Nucleic Acids Res*. 2012;41(D1):D590–D596. doi:10.1093/nar/gks1219
54. Yilmaz P, Parfrey LW, Yarza P, et al. The SILVA and "all-species living tree project (LTP)" taxonomic frameworks. *Nucleic Acids Res*. 2014;42(D1):D643–D648. doi:10.1093/nar/gkt1209
55. Davis NM, Proctor DM, Holmes SP, Relman DA, Callahan BJ. Simple statistical identification and removal of contaminant sequences in marker-gene and metagenomics data. *Microbiome*. 2018;6(1):226. doi:10.1186/s40168-018-0605-2
56. Stamatakis A. RAxML version 8: a tool for phylogenetic analysis and post-analysis of large phylogenies. *Bioinformatics*. 2014;30(9):1312–1313. doi:10.1093/bioinformatics/btu033
57. Shannon CE. A mathematical theory of communication. *Bell Syst Tech J*. 1948;27(3):379–423. doi:10.1002/j.1538-7305.1948.tb01338.x
58. Faith DP. Conservation evaluation and phylogenetic diversity. *Biol Conserv*. 1992;61(1):1–10. doi:10.1016/0006-3207(92)91201-3
59. McMurdie PJ, Holmes S. phyloseq: an R package for reproducible interactive analysis and graphics of microbiome census data. *PLoS One*. 2013;8(4):e61217. doi:10.1371/journal.pone.0061217
60. Kembel SW, Cowan PD, Helmus MR, et al. Picante: r tools for integrating phylogenies and ecology. *Bioinformatics*. 2010;26(11):1463–1464. doi:10.1093/bioinformatics/btq166
61. Lozupone C, Knight R. UniFrac: a new phylogenetic method for comparing microbial communities. *Appl Environ Microbiol*. 2005;71(12):8228–8235. doi:10.1128/AEM.71.12.8228-8235.2005
62. Oksanen J, Blanchet FG, Kindt R, et al. Package 'vegan'. *Community Ecology Package Version*. 2013;2(9):1–295.
63. Anderson MJ. Permutational multivariate analysis of variance (PERMANOVA). *Wiley StatsRef*. 2014;1–15.
64. Kaul A, Mandal S, Davidov O, Peddada SD. Analysis of microbiome data in the presence of excess zeros. *Front Microbiol*. 2017;8:2114. doi:10.3389/fmicb.2017.02114
65. Love MI, Huber W, Anders S. Moderated estimation of fold change and dispersion for RNA-seq data with DESeq2. *Genome Biol*. 2014;15(12):1–21. doi:10.1186/s13059-014-0550-8
66. Lozupone C, Lladser ME, Knights D, Stombaugh J, Knight R. UniFrac: an effective distance metric for microbial community comparison. *ISME J*. 2011;5(2):169–172. doi:10.1038/ismej.2010.133
67. Farhadipour M, Depoortere I. The function of gastrointestinal hormones in obesity—implications for the regulation of energy intake. *Nutrients*. 2021;13(6):1839. doi:10.3390/nu13061839

68. Izquierdo AG, Crujeiras AB, Casanueva FF, Carreira MC. Leptin, obesity, and leptin resistance: where are we 25 years later? *Nutrients*. 2019;11(11):2704. doi:10.3390/nu11112704
69. Torekov SS, Madsbad S, Holst JJ. Obesity – an indication for GLP-1 treatment? Obesity pathophysiology and GLP-1 treatment potential. *Obes Rev*. 2011;12(8):593–601. doi:10.1111/j.1467-789X.2011.00860.x
70. Makris MC, Alexandrou A, Papatsoutsos EG, et al. Ghrelin and Obesity: identifying Gaps and Dispelling Myths. A Reappraisal. *Vivo*. 2017;31(6):1047.
71. Lee W-J, Chong K, Ser K-H, et al. C-peptide predicts the remission of type 2 diabetes after bariatric surgery. *Obes Surg*. 2012;22(2):293–298. doi:10.1007/s11695-011-0565-0
72. Malesza IJ, Malesza M, Walkowiak J, et al. High-fat, western-style diet, systemic inflammation, and gut microbiota: a narrative review. *Cells*. 2021;10(11):3164. doi:10.3390/cells10113164
73. Wilson AS, Koller KR, Ramaboli MC, et al. Diet and the human gut microbiome: an international review. *Dig Dis Sci*. 2020;65(3):723–740. doi:10.1007/s10620-020-06112-w
74. Wolters M, Ahrens J, Romaní-Pérez M, et al. Dietary fat, the gut microbiota, and metabolic health – a systematic review conducted within the MyNewGut project. *Clin Nutr*. 2019;38(6):2504–2520. doi:10.1016/j.clnu.2018.12.024
75. van Rutte PWJ, Nienhuijs SW, Jakimowicz JJ, van Montfort G. Identification of technical errors and hazard zones in sleeve gastrectomy using OCHRA. *Surg Endosc*. 2017;31(2):561–566. doi:10.1007/s00464-016-4997-4
76. Khalid SI, Maasarani S, Shanker RM, Becerra AZ, Omotosho P, Torquati A. Social determinants of health and their impact on rates of postoperative complications among patients undergoing vertical sleeve gastrectomy. *Surgery*. 2022;171(2):447–452. doi:10.1016/j.surg.2021.06.023
77. Sinclair P, Docherty N, le Roux CW. Metabolic effects of bariatric surgery. *Clin Chem*. 2018;64(1):72–81. doi:10.1373/clinchem.2017.272336
78. Batterham RL, Cummings DE. Mechanisms of diabetes improvement following bariatric/metabolic surgery. *Diabetes Care*. 2016;39(6):893–901. doi:10.2337/dc16-0145
79. Wang W, Mei A, Qian H, et al. The role of glucagon-like peptide-1 receptor agonists in chronic obstructive pulmonary disease. *Int J Chron Obstruct Pulmon Dis*. 2023;Volume 18:129–137. doi:10.2147/COPD.S393323
80. Viby N-E, Isidor MS, Buggeskov KB, Poulsen SS, Hansen JB, Kissow H. Glucagon-like peptide-1 (GLP-1) reduces mortality and improves lung function in a model of experimental obstructive lung disease in female mice. *Endocrinology*. 2013;154(12):4503–4511. doi:10.1210/en.2013-1666
81. Fandiño J, Toba L, González-Matías LC, Diz-Chaves Y, Mallo F. GLP-1 receptor agonist ameliorates experimental lung fibrosis. *Sci Rep*. 2020;10(1):18091. doi:10.1038/s41598-020-74912-1
82. Enaud R, Prevel R, Ciarlo E, et al. The gut-lung axis in health and respiratory diseases: a place for inter-organ and inter-kingdom crosstalks. mini review. *Front Cell Infect Microbiol*. 2020;10(9). doi:10.3389/fcimb.2020.00009
83. Martin AM, Sun EW, Rogers GB, Keating DJ. The influence of the gut microbiome on host metabolism through the regulation of gut hormone release. mini review. *Front Physiol*. 2019;10. doi:10.3389/fphys.2019.00428
84. Fusco W, Lorenzo MB, Cintoni M, et al. Short-chain fatty-acid-producing bacteria: key components of the human gut microbiota. *Nutrients*. 2023;15(9):2211. doi:10.3390/nu15092211
85. Topping DL, Clifton PM. Short-chain fatty acids and human colonic function: roles of resistant starch and nonstarch polysaccharides. *Physiol Rev*. 2001;81(3):1031–1064. doi:10.1152/physrev.2001.81.3.1031
86. Daniele B, Andrew BT, Graeme M, Catherine EM. The pharmacology and function of receptors for short-chain fatty acids. *Mol Pharmacol*. 2016;89(3):388. doi:10.1124/mol.115.102301
87. Huang M-T, Chiu C-J, Tsai C-Y, et al. Short-chain fatty acids ameliorate allergic airway inflammation via sequential induction of PMN-MDSCs and treg cells. *J Allergy Clin Immunol*. 2023;2(4):100163. doi:10.1016/j.jacig.2023.100163
88. Cait A, Hughes MR, Antignano F, et al. Microbiome-driven allergic lung inflammation is ameliorated by short-chain fatty acids. *Mucosal Immunol*. 2018;11(3):785–795. doi:10.1038/mi.2017.75
89. Chen J, Chen X, Ho CL. Recent development of probiotic bifidobacteria for treating human diseases. *Front Bioeng Biotechnol*. 2021;9:770248. doi:10.3389/fbioe.2021.770248
90. Sorbara MT, Littmann ER, Fontana E, et al. Functional and genomic variation between human-derived isolates of Lachnospiraceae reveals inter-and intra-species diversity. *Cell Host Microbe*. 2020;28(1):134–146.e4. doi:10.1016/j.chom.2020.05.005
91. Ju T, Kong JY, Stothard P, Willing BP. Defining the role of Parasutterella, a previously uncharacterized member of the core gut microbiota. *ISME J*. 2019;13(6):1520–1534. doi:10.1038/s41396-019-0364-5
92. O'Callaghan A, Van Sinderen D. Bifidobacteria and their role as members of the human gut microbiota. *Front Microbiol*. 2016;7:206360.
93. Schellekens H, Torres-Fuentes C, van de Wouw M, et al. Bifidobacterium longum counters the effects of obesity: partial successful translation from rodent to human. *EBioMedicine*. 2021;63:103176. doi:10.1016/j.ebiom.2020.103176
94. Raftis EJ, Delday MI, Cowie P, et al. Bifidobacterium breve MRx0004 protects against airway inflammation in a severe asthma model by suppressing both neutrophil and eosinophil lung infiltration. *Sci Rep*. 2018;8(1):12024. doi:10.1038/s41598-018-30448-z
95. McCumber AW, Kim YJ, Granek J, Tighe RM, Gunsch CK. Soil exposure modulates the immune response to an influenza challenge in a mouse model. *Sci Total Environ*. 2024;922:170865. doi:10.1016/j.scitotenv.2024.170865
96. Vacca M, Celano G, Calabrese FM, Portincasa P, Gobbetti M, De Angelis M. The Controversial Role of Human Gut Lachnospiraceae. *Microorganisms*. 2020;8(4):573. doi:10.3390/microorganisms8040573
97. Wei X, Tao J, Xiao S, et al. Xiexin Tang improves the symptom of type 2 diabetic rats by modulation of the gut microbiota. *Sci Rep*. 2018;8(1):3685. doi:10.1038/s41598-018-22094-2
98. Lan Y, Ning K, Ma Y, et al. High-density lipoprotein cholesterol as a potential medium between depletion of lachnospiraceae genera and hypertension under a high-calorie diet. *Microbiology Spectrum*. 2022;10(6):e02349–22. doi:10.1128/spectrum.02349-22
99. Connors J, Dawe N, Van Limbergen J. The role of succinate in the regulation of intestinal inflammation. *Nutrients*. 2018;11(1):25. doi:10.3390/nu11010025
100. Henneke L, Schlicht K, Andreani NA, et al. A dietary carbohydrate – gut Parasutterella – human fatty acid biosynthesis metabolic axis in obesity and type 2 diabetes. *Gut Microbes*. 2022;14(1):2057778. doi:10.1080/19490976.2022.2057778

101. Chen Y-J, Wu H, Wu S-D, et al. Parasutterella, in association with irritable bowel syndrome and intestinal chronic inflammation. *J Gastroenterol Hepatol*. 2018;33(11):1844–1852. doi:10.1111/jgh.14281
102. Gu Y, Liu C, Zheng N, Jia W, Zhang W, Li H. Metabolic and gut microbial characterization of obesity-prone mice under a high-fat diet. *J Proteome Res*. 2019;18(4):1703–1714. doi:10.1021/acs.jproteome.8b00945
103. Morales-Marroquin E, Hanson B, Greathouse L, de la Cruz-Munoz N, Messiah SE. Comparison of methodological approaches to human gut microbiota changes in response to metabolic and bariatric surgery: a systematic review. *Obes Rev*. 2020;21(8). doi:10.1111/obr.13025